INFORMATION TO USERS

This manuscript has been reproduced from the microfilm master. UMI films the text directly from the original or copy submitted. Thus, some thesis and dissertation copies are in typewriter face, while others may be from any type of computer printer.

The quality of this reproduction is dependent upon the quality of the copy submitted. Broken or indistinct print, colored or poor quality illustrations and photographs, print bleedthrough, substandard margins, and improper alignment can adversely affect reproduction.

In the unlikely event that the author did not send UMI a complete manuscript and there are missing pages, these will be noted. Also, if unauthorized copyright material had to be removed, a note will indicate the deletion.

Oversize materials (e.g., maps, drawings, charts) are reproduced by sectioning the original, beginning at the upper left-hand corner and continuing from left to right in equal sections with small overlaps.

Photographs included in the original manuscript have been reproduced xerographically in this copy. Higher quality 6" x 9" black and white photographic prints are available for any photographs or illustrations appearing in this copy for an additional charge. Contact UMI directly to order.

Bell & Howell Information and Learning
300 North Zeeb Road, Ann Arbor, MI 48106-1346 USA
800-521-0600

Université d'Ottawa · University of Ottawa

Morphological and Spectroscopic Study of Human Neuroblastoma IMR-32 Cell Differentiation

Vanisree Kathiravan

Thesis submitted to the Department of Biochemistry, Microbiology and Immunology in partial fulfillment of the requirements for the degree of Master of Science.

University of Ottawa
Ottawa, Ontario, Canada
April 1999

ABSTRACT

Neuroblastoma is a childhood tumor for which treatment is unsuccessful in a vast majority of patients despite the introduction of very intense and demanding treatment regimens. All-*trans* retinoic acid (tRA) and 8-bromo-adenosine-3':5'-cyclic monophosphate (cAMP) have been shown to inhibit proliferation, induce cell differentiation and reverse malignant phenotype of a variety of neuroblastoma cell types *in vitro*. In this thesis, we chose IMR-32 human neuroblastoma cell line because it exhibits two of the main defects found in neuroblastoma: N-myc gene amplification and defective high affinity NGF receptor Trk-A.

Treated IMR-32 cells were analyzed for alterations in cell growth and cell morphology. The morphological differentiation induced by cAMP and tRA is accompanied by a decrease in cell proliferation rate. In the course of the study we also investigated the effect of the two differentiation inducers on the expression and distribution of neurofilament (NF) proteins in the IMR-32 cell line. We observed a gradual increase in the intensity of 68 kDa, 200 kDa and 150 kDa subunits of NF protein during the progress of differentiation.

Diagnosis of various other cancers by studying the structural changes at the molecular level using Fourier Transform Infrared Spectroscopy (FTIR) is well established. The main objective of this thesis work was to determine whether diagnostic bands in FTIR spectrum reflect the mitotic ability of IMR-32 cells and whether treatment with tRA and cAMP induces spectral changes characteristic of normal cells.

The main results of this study indicate that the differentiated IMR-32 cells exhibited no spectral changes in the phosphate stretching region compared to proliferating cells, in spite of minor spectral alterations in the bands used to characterize the secondary structure of protein, more specifically the amide I band. The changes in this protein band reflect the differentiation progress. Seven days after treatment, the cells exited the cell cycle and remained quiescent over the following three weeks. However, no change in the phosphate stretching region was observed.

Observations in the phosphate stretching region reflect the cell proliferative ability in spite of treatment. Drastic cytosolic molecular modifications due to differentiation (changes in the expression level of NSE, CAT, TH, NF and trk-A) are reflected by amide I band changes in the FTIR spectra. These results suggest that FTIR based diagnostic test could be used to monitor chemotherapy treatment.

Dedication

This thesis is dedicated to my loving family: husband Kathir, son Mugil, sister and parents.

Acknowledgements

I would like to gratefully acknowledge the valuable advice and support provided by :

Dr. Danielle Carrier, for offering me the opportunity to join the Graduate program at University of Ottawa. Further I am indebted to her for motivating me to work in spectroscopy. Her continued interest and critical views of my work helped in the development of this thesis.

Dr. Jenny Phipps, of NRC, who provided me not only with the facilities for research in her lab but also on- going support and motivation to complete this project successfully.

Dr. Patrick Wong, a pioneer in the area of study of cancer using spectroscopic techniques, who, in spite of his busy schedule, spent valuable time in advising me on spectral analysis and instilled confidence in me to carry out this work.

Mrs. Pascale Jaklis, Technician with Dr. Wong, for introductory help and initial training to use spectroscopy in the lab.

Ms. Loubaba Belbaraka, who helped me in various aspects of cell culture when I joined Dr. Phipps' lab.

Dr. Harve' Jouishomme, for helping me with flow cytometry.

Dr. Saba Siddiqi, for specific help with the Western blot technique and general encouragement and advice during the course of the work.

Mr. Maroun Bou Khalil, a colleague of mine, for useful discussions and clarifications on infrared spectroscopy technique.

My friends Nathalie and Prachi, for their moral support.

Dr. Sattar and his lab members, especially Makonnen Abebe.

Dr. Yudi Singh and his family members, for their loving support.

TABLE OF CONTENTS

LIST OF FIGURES

LIST OF TABLES

LIST OF ABBREVIATIONS

ACTH	Adrenocorticotrophic hormone
BE	β-endorphin
bFGF	Basic fibroblast growth factor
BSA	Bovine serum albumin
BDNF	Brain-derived neurotrophic factor
8-bromo-cAMP[a]	8-bromo-adenosine-3':5'-cyclic monophosphate
CRABP	Cellular retinoic acid binding proteins
CNS	Central nervous system
CAT	Choline acetyl transferase
CDF	Choline acetyl transferase development factor
cRA	*Cis*-retinoic acid
9-cis-RA	9-*cis*-retinoic acid
13-cis-RA	13-*cis*-retinoic acid
CRF	Corticotropin releasing factor
D_2O	Deuterated water
dbcAMP	Dibutyryl cyclic adenosine monophosphate
DMSO	Dimethyl sulfoxide
FACS	Fluorescent activated cell sorter
FBS	Fetal bovine serum
FTIR	Fourier transform infrared spectroscopy
IGF-II	Insulin like growth factor-II
IL	Interleukins
KRS-5	Thallium bromide iodide
MEM	Minimum essential medium
MDR1	Multidrug resistance gene
NGF	Nerve growth factor
NCAM	Neural cell adhesion molecules
NB	Neuroblastoma
NF	Neurofilament
NSE	Neuron specific enolase

PMSF	Phenyl methyl sulfonyl fluoride
PBS	Phosphate buffered saline
PBS-BSA	Phosphate buffered saline containing 1% bovine serum albumin
PCNA	Proliferating cell nuclear antigen
POMC	Proopiomelanocortin
PI	Propidium iodide
PNS	Peripheral nervous system
RA	Retinoic acid
RAR	Retinoic acid receptors
RXR	Retinoid X receptors
SDS	Sodium dodecyl sulfate
SDS-PAGE	Sodium dodecyl sulfate polyacryl amide gel electrophoresis
tRA	All-*trans* retinoic acid
TPA	12-O-tetradecanoyl phorbol 13-acetate
TBS	Tris-buffered saline
TBST	10 mM Tris (pH8.0), 150 mM NaCl and 0.05% (v/v) Tween-20
TH	Tyrosine hydroxylase
trk-A	High affinity nerve growth factor receptor
VIP	Vasoactive intestinal polypeptide

a. Referred shortly as cAMP throughout this thesis.

CHAPTER 1

INTRODUCTION

1.1 Neuroblastoma

Human neuroblastoma (NB) is a tumor of the peripheral nervous system (PNS) and is thought to arise from migratory cells of the embryonal neural crest. This tumor develops in tissues of a sympathetic neural origin, such as the adrenal gland. In advanced disease, it metastasizes to many tissues including the liver, bone and bone marrow (Brodeur *et al.*, 1993). This embryonal tumor of neural crest origin shows an extraordinary clinical and biological heterogeneity which suggests that its biology is closely related with the developmental stage of the neurons from which the tumor originates. The clinical outcome ranges from differentiation to ganglioneuroma, or regression due to differentiation or apoptosis after no or minimal therapy in the most favorable subset, to tumor progression and poor clinical outcome despite intensive therapy in the most unfavorable subset (Kogner *et al.*, 1997). The biological mechanisms underlying these changes are unknown. The similarities of many NB tumor cells to neural-crest cell types suggest that NB results from a block in the differentiation of neural-crest precursor cells during development (Cooper *et al.*, 1990; Helman *et al.*, 1987). This phenomenon has, however, stressed the importance of the finding that some neuroblastoma cell lines will differentiate spontaneously *in vivo* and *in vitro* under the influence of certain inducers. One study suggests that neuroblastomas which progress on or after chemotherapy could result from altered expression of drug resistance genes, tumor cells in 'sanctuary' sites of low drug penetration, tumor hypoxia, tumor cells

resting out of cell cycle or all of the above. No current experimental data favors any of the above mechanisms, except that the poor response of relapsed neuroblastoma to further therapy suggests that selection for tumor cells with genetic alterations conferring drug resistance plays a key role (Keshelava *et al.*, 1997).

Examination of tumor specimens from patients with advanced NB has revealed that over 30% exhibit amplification and over-expression of the N-myc oncogene G (Brodeur, 1991), which is associated with the progression and metastatic nature of NB (Schwab *et al.*, 1985). Neuroblastoma has a particularly poor prognosis (<30% survival) in patients older than 2 years of age at diagnosis, advanced stage disease and/or disease characterized by N-myc gene amplification. By contrast, low-stage neuroblastoma patients diagnosed at less than 2 years of age and those tumors with a single copy N-myc are cured more than 75% of the time. Furthermore, there is also a unique advanced stage neuroblastoma which occurs in infants under 1 year of age, stage 4S, that shows a remarkably high spontaneous regression rate, nearly 100 times that of any other human cancer. This suggests that at least one form of neuroblastoma may exhibit delayed onset of apoptosis or/and do differentiate by a mechanism that remains to be defined (Schmidt *et al.*, 1997).

There are numerous reports of spontaneous regression of NB tumors. Several mechanisms have been proposed to account for this phenomenon: 1) activation of a host mediated anti-NB tumor response; 2) induction of programmed cell death and 3) induction of terminal differentiation (Lucarelli *et al.*, 1994). The induction chemotherapy included all-*trans* and *cis*-retinoic acid (tRA or cRA) associated or not with doxorubicin, vincristine, and cyclophosphamide or in some patients with cis-platinum and etoposide as previously reported (Hartmann *et al*, 1988).

A major characteristic of human neuroblastoma cells *in vivo* and *in vitro* is their capacity to differentiate into more mature cell types representative of those constituting the neural crest (Spengler *et al.*, 1994). The ability of some NB tumor cell lines to differentiate *in vitro* provides a model system to study the molecular events regulating cell growth and differentiation of these neural crest cell derivatives and may provide insights into the molecular mechanisms contributing to their tumorigenic conversion (Thiele, 1991). Although these cells already show several characteristics of neuronal cells, they undergo major morphological, biochemical and functional changes following exposure to differentiating agents (Vignali *et al.*, 1996).

1.2 Types of Neuroblastoma Cell Line

Human neuroblastoma cell lines in culture frequently comprise multiple cell types. Most prominent are neuroblastic (N) cells, small, rounded cells with short neuritic processes which grow as poorly attached aggregates and contain the neurotransmitter biosynthetic enzymes and uptake mechanisms of embryonic neuronal precursors (Ciccarone *et al.*, 1989). A second, flattened cell type, termed S for its substrate adhesiveness, has cytoplasmic and cell surface proteins suggestive of a Schwann/glial/ melanocyte or ectomesenchymal precursor cell (Ross *et al.*, 1983; Rettig *et al.*, 1987). A third type (I) is intermediate in morphology and has biochemical characteristic of both N and S cells. Differentiation occurring spontaneously or induced by exogenous agents can proceed towards either a neuronal (Nrl) or non-neuronal neural crest lineage, as previously reported (Ross *et al.*, 1983; Ross *et al.*, 1991). I-type cells are thought either to represent multipotent precursors that give rise to either N- or S-type cells, or to be

transitional cells during the phenotypic interconversion (transdifferentiation) between N and S. Transdifferentiation between the S and N phenotypes is frequently observed *in vitro*. The functional correlates of the two phenotypes is poorly understood. Thus human neuroblastoma cell lines provide a system for evaluation of potential for differentiation along two (or more) lineages. IMR-32 cell line used in our study contains a large majority of N-type cells and a few I-type cells.

1.3 Induction of Differentiation

Despite a number of genetic alterations (including a deletion in chromosome 1p, amplification of N-myc and loss of heterozygosity at a number of genetic loci), treatment with biological response modifiers reverts the malignant phenotype of NB cells and induces them to express genes characteristic of different neural crest cell lineages, such as neuronal cells, adrenal medulla cells, and melanocytes (Gaetano *et al.*, 1992).

Differentiation may occur spontaneously or in response to a diverse group of chemical agents. The ability of neuroblastoma cells to differentiate *in vitro* and *in vivo* suggests the possibility of new therapeutic approaches using differentiation inducing agents (Li *et al.*, 1994). A variety of chemicals and biologic-response modifiers are known to induce morphological, biochemical, ultrastructural and electrophysiological differentiation of NB cell lines. *In vitro*, a number of agents can induce NB to differentiate, presumably by activating distinct biochemical signal transduction pathways.

A variety of agents have been shown to induce differentiation of human neuroblastoma *in vitro*, including retinoic acid (Sidell, 1982), cyclic AMP elevating agents (Prasad and Kumar, 1975; Lando *et al.*, 1990), bromodeoxyuridine (Prasad *et al.*,

1973), interferons (Pedersen *et al.*, 1993) and 12-O-tetradecanoyl phorbol 13-acetate (TPA) (Pahlman *et al.*, 1981). The availability of such substances encouraged testing to show whether one therapeutic strategy for this tumor might involve induction of differentiation, thereby interfering with tumor growth. One of the most potent differentiation inducers for human neuroblastoma *in vitro* is retinoic acid (Reynolds *et al.*, 1991). Retinoic acid (RA) has been reported to induce differentiation of neuroblastoma cells under experimental conditions *in vitro* and *in vivo* (Kogner *et al.*, 1994). In some NB cell lines, such as LA-N-1 and LA-N-5, RA has been shown to arrest cell growth and induce the development of a variety of morphological, electrophysiological, ultra structural and biochemical properties characteristic of normal differentiated neuronal cells. Morphological differentiation of NB by tRA (all-*trans* retinoic acid) was first reported by Sidell (Sidell, 1982). Subsequent studies demonstrated biochemical differentiation, based on the increased acetylcholinesterase activity and on electrophysiological differentiation (Sidell *et al.*, 1984, 1985).

1.4 Cell Differentiation

The human neuroblastoma cell model permits the characterization of cell differentiation along discrete pathways in normal neural crest development (Biedler *et al.*, 1991). This model recapitulates the stages of differentiation of sympathetic neurons during embryonic development, as illustrated diagrammatically in Figure 1.1.

Figure 1.1 Model of human neuroblastoma cell differentiation and transdifferentiation (Biedler *et al.*, 1991).

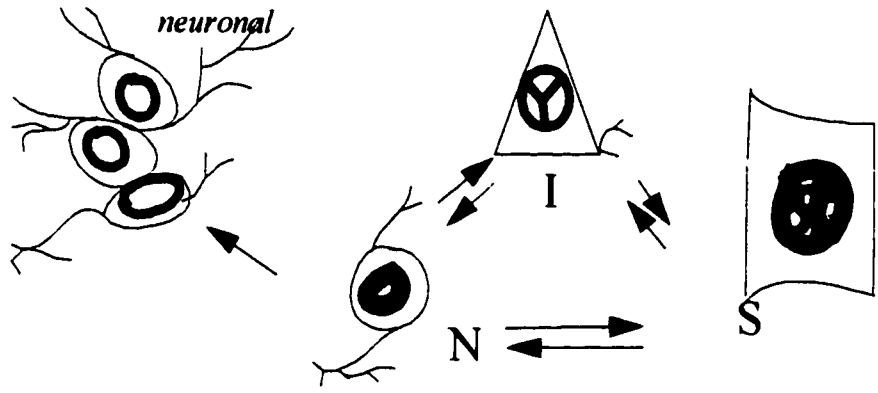
neuronal
I
N
S

1.5 Retinoids in Neuroblastoma Therapy

All *trans* retinoic acid (tRA) and its analogs, 13-*cis*-retinoic acid (13-*cis*-RA) and 9-*cis*-retinoic acid (9-*cis*-RA) have shown anti-neuroblastoma activity in a variety of malignancies. The chemical structure of all-*trans* retinoic acid is shown in Figure 1.2.

Retinoic acid (RA) is a naturally occurring retinoid that can induce growth inhibition and cellular differentiation in a wide variety of malignant cell types, including neuroblastoma. In neuroblastoma, 13-*cis* and all-*trans*-retinoic acid have been used clinically on the basis of *in vitro* data demonstrating their ability to induce neuroblastoma differentiation. Phase 1 clinical trials have shown that 13-*cis*-RA is better tolerated than *trans*-RA, especially in children (Reynolds *et al.*, 1994). The maximum tolerated dose for 13-*cis*-RA in children using an intermittent schedule (14 days on/14 days rest) is 160 mg/m^2/day, while the maximum tolerated dose for *trans*-RA in children is 60 mg/m^2/day. There are also differences in pharmacokinetics of the 2 drugs: the half-life of 13-*cis*-RA is 5 hrs compared to 45 minutes for *trans*-RA, peak plasma levels differ (7.4 μM for 13-*cis*-RA, 0.6 μM for *trans*-RA), and unlike 13-*cis*-RA, *trans*-RA clearance rapidly increases during treatment resulting in a large fall of drug levels and area under the time-concentration curve. Thus at clinically achievable drug levels, 13-*cis*-RA is as effective or more effective than *trans*-RA in producing prolonged growth arrest of neuroblastoma *in vitro* (Reynolds *et al.*, 1994). However, sustained remission rates in clinical trials have so far been disappointing. Recent *in vitro* and animal studies have shown that 9-*cis*-retinoic acid is more effective than the all-*trans* isomer for inducing cell differentiation, inhibiting proliferation and preventing chemically-induced cancers (Lovat *et al.*, 1997). In addition to inducing morphological differentiation of many cultured NB cell lines, RA

Figure 1.2 Structure of all *trans* retinoic acid (Gudas, 1992).

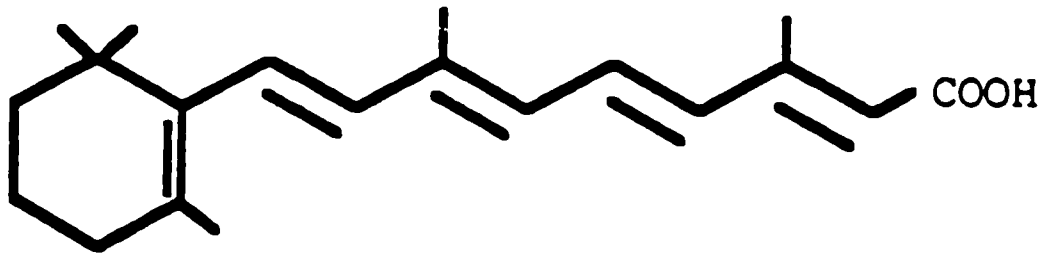
COOH

has also been shown to modulate the expression of a range of genes in such cells and to have anti-NB activity *in vivo* (Haber *et al.*, 1994).

The effects of RA within cells are mediated by at least three classes of proteins, a fact which contributes to the complex biology of retinoid action. Two of these classes, the retinoic acid receptors (RAR) and retinoid X receptors (RXR), are ligand-dependent transcription factors, encoded by the RAR α, β, and γ and RXR α, β, and γ genes, respectively (Gudas, 1992). The two families of nuclear receptors have structural and functional homology not only to each other, but also to the steroid hormone receptor family of transcription factors (Evans, 1988). Nuclear receptors bind to *cis*-acting response elements as dimers, where each receptor recognizes a consensus sequence of 5-6 bases, i.e. rGTTCA or rGGTCA in a similar fashion as estrogen and thyroid hormone receptors. Variability in response to RA may be due to alterations in expression of the receptors for RA. The third class of proteins mediating the effects of RA are the cellular retinoic acid-binding proteins, CRABP1 and 2, which bind cytoplasmic RA with high affinity (Giguere *et al.*, 1990). The concentration of CRABP in the most RA responsive NB cell line (LA-N-5) is approximately twice that in the least responsive NB cell line (CHP 100) (Sidell *et al.*, 1984). There have been a number of studies which have suggested that high levels of CRABP are involved in mediating resistance to RA, by binding to this compound and preventing its delivery to the nucleus (e.g. Boylan and Gudas, 1991). A detailed understanding of the effect of retinoic acid on neuroblastoma cells *in vitro* and *in vivo* requires further analysis of these receptors and also of retinoic acid-responsive genes.

Expression of N-myc (Schwab *et al.*, 1983), a key oncogene in NB, has been reported to be down-regulated by RA prior to morphological differentiation (Thiele *et al.*, 1985). Neuronal differentiation induced by RA treatment is associated with an increase in multidrug resistance gene (MDR1) mRNA in some NB cell lines (Bates *et al.*, 1989). Some studies indicate that the inability of RA to arrest growth of some NB cells or the development of RA resistance in RA treated cell cultures may be associated with the expression of high levels of insulin like growth factor-II (IGF-II) (Gaetano *et al.*, 1991) and suggest that competitive molecular mechanisms may be responsible for the arrest of cell growth and induction of differentiation versus the maintenance of the proliferative state.

N-myc oncogene amplification in neuroblastoma has been found to be significantly associated with advanced stage of the disease and tumor progression. However, there is a lack of data on tumors, regarding the relationship between N-myc gene amplification and proliferation activity. Previous studies have shown that the decrease in N-MYC and MYB (are developmentally regulated proto-oncogenes that encode nuclear binding proteins) expression occurs prior to morphologic differentiation yet is not associated with growth arrest suggesting that regulation of both N-MYC and MYB may be important in the implementation of neuroblast differentiation programs (Thiele, 1991). However, growth arrest of NB cells by either serum starvation or aphidicolin (an inhibitor of DNA polymerase) was not associated with alterations in the expression of N-MYC or MYB mRNA. Furthermore, transfection studies indicate that constitutive expression of either N-MYC or MYB is capable of blocking *in vitro* differentiation.

One study indicates that higher proliferating cell nuclear antigen (PCNA, an auxiliary component of DNA polymerase δ) levels occur in tumors with an amplified N-myc gene relative to tumors with a single N-myc gene, and in metastatic relative to non-metastatic tumors (Keim *et al.*, 1993). In three different cell lines (Human neuroblastoma SH-SY-5Y, IMR-32 cells and rat phaeochromocytoma PC-12 cells), the acquisition of a mature neuronal phenotype is accompanied by an increase in the expression of neuronal, but not of ubiquitous kinesin (Vignali *et al.*, 1996). Pedersen *et al.* (1993) showed that in human NB cells, a redistribution of peripherin from a perinuclear position to the neurites is observed when these cells are induced with dibutyryl cyclic adenosine monophosphate (dbcAMP) and tRA.

1.6 Neurotrophin Receptors and their Role in the Differentiation Process

The expression of a functional nerve growth factor (NGF) receptor is important in mediating the ability of neuroblastoma cells to undergo neuronal differentiation, and possibly programmed cell death associated with neurotrophin deprivation. Recent studies have revealed that growth, differentiation and survival of neural crest-derived cells are strongly regulated by neurotrophins and their receptors (Nakagawara and Brodeur, 1997).

The nerve growth factor was the first neurotrophin to be identified and it is the prototype of a family of homologous neurotrophins that includes brain-derived neurotrophic factor (BDNF), neurotrophin-3 (NT-3) and neurotrophin-4/-5 (NT-4/NT-5). These factors have important roles in growth, survival and differentiation of specific types of neurons of the peripheral and central nervous system. Neurotrophic factors bind to specialized cell surface receptors. Analysis of the ligand-receptor interactions has

shown that trk-A is a receptor for NGF and NT-3, trk-B is a receptor for BDNF as well as NT-4 and NT-3 and trk-C is a receptor for NT-3 (Nakagawara and Brodeur, 1997). Two types of NGF receptors have been identified, namely a low-affinity (gp75NGFR) and a high affinity (trk-A) receptor (Chao, 1992). The binding of NGF to its high affinity receptor triggers a series of early, intermediate, and late effects which contribute to neuronal survival and differentiation (Figure 1.3). For example, transcription of the proto-oncogene, c-fos, is induced within 30 minutes, specific activity of ornithine decarboxylase rises within a few hours (6-7 hours), and synthesis of such neuronal differentiation markers as neurofilament peptides and sodium channels is induced after several weeks of exposure (Reddy *et al.*, 1991).

The majority of primary neuroblastomas express trk-A (Nakagawara *et al.*, 1992; Nakagawara *et al.*, 1993), and at least some of these are able to respond to NGF by undergoing terminal differentiation. Furthermore, NGF deprivation may lead to programmed cell death (Nakagawara *et al.*, 1993). High levels of trk-A expression are associated with favorable outcome in NB, and low or absent expression of this gene is frequently associated with N-myc gene amplification, an adverse prognostic indicator (Nakagawara *et al.*, 1993).

One study has reported that lack of expression of gp140trk-A mRNA in neuroblastomas, whether or not the N-myc proto-oncogene was amplified, was associated with poor survival. Conversely, expression of gp140trk-A generally correlated with excellent survival (Suzuki *et al.*, 1993). However, a small group of patients did not survive even though their tumors expressed gp140trk-A and did not have amplification of N-myc (Suzuki *et al.*, 1993). An increase in the number of receptors for the nerve growth

Figure 1.3 Schematic representation of the biochemical actions of NGF on responsive cells (Reddy *et al.*, 1991).

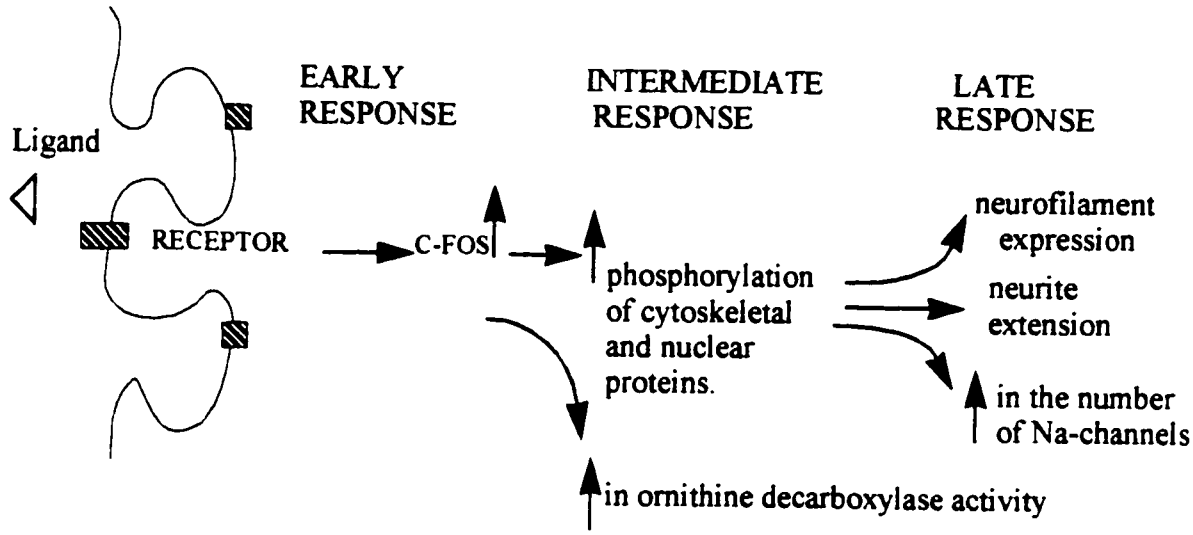
EARLY
RESPONSE
INTERMEDIATE
RESPONSE
LATE
RESPONSE
Ligand
RECEPTOR
C-FOS
phosphorylation
of cytoskeletal
and nuclear
proteins.
neurofilament
expression
neurite
extension
in the number
of Na-channels
in ornithine decarboxylase activity

factor (NGF) was reported to be associated with neuroblastoma differentiation following RA treatment.

The trk-A gene encodes a membrane-bound receptor with an intracellular tyrosine kinase which, following ligand binding, rapidly autophosphorylates the receptor. Thus trk-A shares similar functional mechanisms with other classical growth factor receptors. The role of gp75NGFR in the trk-A-mediated NGF signal is not fully understood and evidence has been presented that the low-affinity receptor is dispensable.

Several groups have found the expression of high levels of trk-A to be correlated with good prognosis, while constitutive expression of BDNF and variable expression of trk-B are associated with poor prognosis. Activation of the BDNF-trk-B signal transduction promoted cell survival and neurite outgrowth (Lucarelli *et al.*, 1997).

Early studies of differentiation of human neuroblastoma cell lines demonstrated NGF-induced neurite extension and upregulation of neural markers (Perez-Polo *et al.*, 1979; Sonnenfeld and Ishii, 1982). An important disagreement between these articles is the effect of NGF on the rate of cell growth. Perez-Polo *et al.* (1979) reported that the neuroblastoma cells ceased multiplying, but Sonnenfeld and Ishii (1982) found little or no effect on the rate of cell growth.

Distinct defects have been identified in the NGF receptor pathway in human NB cell lines (Azar *et al.*, 1990), and these defects are likely to be important in the initiation and maintenance of the undifferentiated state of NB.

The extension of neurites in responsive human NB cell lines is accompanied by up-regulation in neurofilament (NF) mRNA expression following treatment with NGF (Chen *et al.*, 1990) and retinoic acid (Di Martino *et al.*, 1990). However, the majority of human

NB cell lines do not respond to nerve growth factor (NGF) by extending neurites (Chen *et al.*, 1990). Among the agents capable of inducing differentiation, only RA (and to a lesser extent cAMP) induced a consistent modulation of neurotrophin receptors in NB cell lines.

1.7 Effect of Retinoic Acid on Neuroblastoma Cells *In Vitro*

1.7.1 Neuronal Differentiation

Neuroblastoma cells differentiate toward a neuronal phenotype upon exposure to retinoic acid. This is shown by the formation of morphologically defined neurites and/or axons. The proportion of cells bearing neuritic processes increases, with a mean of more than one neurite per cell and with a neurite length up to 100 μm. This is accompanied by the synthesis of neuronspecific enzymes (such as acetylcholinesterase), neurotransmitters (such as catecholamines) and profound changes in the intermediate filaments (such as neurofilaments) (Melino *et al.*, 1997).

1.7.2 Growth Retardation

The growth of neuroblastoma cell lines is modulated by retinoids (Lotan *et al.*, 1990). Even though the effective concentration of retinoids for inhibition of tumor cells growth in culture is often pharmacological and not physiological, quite a large number of neuroblastoma cell lines are inhibited considerably at physiological dosage (1 μM for retinol and 10 nM for retinoic acid). The effect is time and dose dependent. DNA-synthesis is suppressed and the cells are normally arrested in the G_1 phase (occasionally in the S phase) of the cell cycle. Changes in the cell cycle occur within 12-24 hours after the addition of retinoids to the culture medium, and growth inhibition can be detected 24-72

hours after treatment. However, the growth retardation may differ considerably among different cell lines. The RA-induced effect on proliferation may be related to a simple, direct growth arrest (or retardation of the cell cycle phases) or to the induction of more specific phenomena, i.e. neuronal differentiation or programmed cell death (Melino *et al.*, 1997).

1.7.3 Growth Factors

Several neuroblastoma cell lines grow continuously in mitogen-free media, produce insulin growth factor-2 (IGF-2) and possess type I IGF receptors that are capable of mediating the mitogenic activity of IGF-2. Moreover type I IGF receptor antagonists block the mitogenic effect of exogenously added IGF-1 and IGF-2 and thus inhibit the growth of these cell lines in mitogen-free media. Therefore IGF-2 is either an autocrine or a paracrine growth factor for neuroblastoma. These data allow us to predict that retinoic acid, in order to inhibit cell growth, should down regulate the IGF-2 expression (Melino *et al.*, 1997). It has been suggested that molecular competition between RA and IGF-2 may lead either to growth arrest and differentiation (induced by RA) or to continuous undifferentiated proliferation (induced by IGF-2) (Gaetano *et al.*, 1991).

1.7.4 Modulation of Adhesion Molecules

The expression of appropriate cell adhesion molecules determines the regulation of cell-cell interactions during nervous system development and maintenance. Cell adhesion molecule expression is differentially regulated in NB, and may be relevant to the neoplastic phenotype and tumorigenicity. RA induces neuronal differentiation with profound changes in ultrastructure. The appearance of neuronal characteristics is

followed by the expression of neural cell adhesion molecules (NCAM), detected by specific monoclonal antibody and mRNAs. In RA treated neuroblastoma cells the 180 kDa NCAM isoform was detectable, but this was not seen in untreated cells. Both the 140 and 120 kDa isoforms are expressed in both control and differentiated cells (Melino *et al.*, 1997).

1.7.5 Neurohormones and Cytokines

Another interesting autocrine growth factor candidate for NB is proopiomelanocortin (POMC), which gene is located in 2p23, the same chromosomal band as N-MYC. POMC is transcribed in the anterior pituitary as a 1.2 kb mRNA and its translation products include the classical anterior pituitary hormones, adrenocorticotrophic hormone (ACTH) and β-endorphin (BE). The POMC gene is also transcribed in other normal non pituitary tissues (De Bold *et al.*, 1988) and neoplastic lesions (Yesner, 1978). Pituitary expression of POMC is largely controlled by hypothalamic production of corticotropin releasing factor (CRF); it may be of interest that NB cell lines can also express CRF transcripts (Usui *et al.*, 1989). NB cells can express POMC mRNA, and expression of the POMC transcript is modulated by RA. However, the relationship between CRF and POMC expression in NB is unknown. A variety of receptors with affinity for BE and BE fragments have been described on neuroblastoma cells. Non-opioid receptors, recognising the COOH terminus of BE, have been described in the human NB cell lines, NMB and IMR-32. Several types of opioid receptors, specific for the amino terminal sequence, have also been documented. Inappropriate production of BE may have direct effects on tumor growth and influence local tumor specific immunity. Some NB cell lines express corticotropin releasing

hormones mRNA and peptide, and the levels of the peptide can be increased by agents which raise intracellular cAMP. Exogenous β-endorphin increases the growth of NB cell lines *in vitro*, although the magnitude of the effect is much less than with IGF-II. There is evidence from earlier studies that the proliferative effects of β-endorphin and other opiates is inhibited by opiate antagonists (Melino *et al.*, 1997).

1.7.6 Expression of Interleukins (IL)

There is a complex interplay between neuroectodermal tumors and the host immune system. Neuroblastoma and melanoma cell lines express various neuropeptides able to interact with the immune system: IL-1α, IL-1β and IL-6. Furthermore, their mRNAs and peptides are modulated during RA-induced differentiation. Neural crest-derived tumors therefore appear to produce a wide range of biologically active peptides. There is already evidence that interleukins can influence the neuropeptide expression. The molecular dialogue between neural crest-derived tumors and tumor infiltrating lymphocytes is therefore complex. Immune products may influence growth and differentiation of the tumors, while peptides produced by the tumor cells may have paracrine effects on local immunity (Melino *et al.*, 1997).

1.7.7 Programmed Cell Death

Cell loss within normal and tumor cells occurs either as necrosis or apoptosis. This latter physiological suicide programme requires an active metabolism and protein synthesis followed by cell volume reduction with an intact membrane and degraded chromatin condensation in discrete masses. Apoptosis is also considered to be genetically programmed under inhibitory control by the *bcl*-2 oncoprotein and is triggered by a

signal(s) via specific receptor(s), such as APO-1 or the Fas antigen. Ultimately the apoptotic signal activates endonuclease(s) causing DNA self-cleavage, resulting, morphologically, in cell shrinkage and hyperchromatic nuclear fragments and, biochemically, in chromatin cleavage into nucleosomal oligomers (DNA ladder) (Koizumi *et al.*, 1995). Recent reports suggest that one gene specifically induced and activated in apoptosis is "tissue transglutaminase". The gene catalyses an acyl-transfer reaction among polypeptide chains, forming ε(γ-glutamyl)lysine and N-N-bis(γ-glutamyl)polyamine isodipeptide linkages (Fesus *et al.*, 1991). These form the insoluble apoptotic body (Piacentini *et al.*, 1991). Transglutaminase is activated by retinoic acid in SK-N-BE(2) cells leading to an increase of 12-fold in the enzyme activity (Melino *et al.*, 1988)

1.8 Effect of Retinoic Acid on Neuroectodermal Cells *In Vivo*

There is a large volume of evidence which indicates that there is an effect of RA on NB *in vitro* and this effect has biological relevance. There is also conclusive scientific evidence which indicates that RA plays an important role in the development of the amphibian limb (Tabin, 1991). Recent evidence suggest that RA plays a central role in the nervous system. Although it had been known for several decades that retinoid deprivation during embryogenesis causes central nervous system (CNS) alteration, it has only been within the last few years that retinoids are being viewed as potentially important modulators of nervous system development. Recent studies indicate that RA synthesis occurs in the spinal cord, basal forebrain and retina, and suggest that it may play a role in the development of these tissues (McCaffery and Drager, 1994). RA provides a

polarizing activity in a restricted region of the developing CNS, the floor plate, but not in other CNS regions and mimicks the Zone of Polarizing Activity in limb development. The floor plate also synthesizes RA and 3,4-didehydroretinal (Wagner *et al.*, 1990). Modifications identical to the physiological formation of the neuroectoderm with its anterior-posterior polarity are also induced by RA (Sharpe, 1991). Both in limb and CNS development, homeobox-containing genes are an important class of genes whose expression pattern is altered by exposure to RA and affects the correct spatial-temporal orientation. In both morphologically differentiated and undifferentiated cells, RA induces the expression of Hox C6, D8 and D1 in a variety of neuroblastoma cell lines tested. These changes in gene expression may occur within a few hours of RA treatment and it may be a necessary pre-requisite but not an absolute guarantee of neurite induction (Manohar *et al.*, 1994). RA shows neurotransmitter-specific effects on developing CNS neurons by increasing the survival of cholinergic neurons without affecting that of GABAergic neurons nor interferring with the RA-induced neuritic outgrowth (Waring and Sidell, 1991). Other studies have been conducted to address the question of the distribution of specific proteins such as CRABP, RARα and RXR in developing mammalian CNS. Recent studies using cultured cells show that RA controls neuronal NGF-dependent survival and differentiation (Melino *et al.*, 1997).

1.9 IMR-32 Cell Line

In the recent past, our laboratory has been involved in the study of the effect of all-*trans*-retinoic acid (tRA) on the human neuroblastoma cell line IMR-32 to explore the *in vitro* differentiation of neuroblastoma cell lines. IMR-32 cell line is a very aggressive

tumor phenotype exhibiting two of the main defects found in neuroblastoma: N-myc gene amplification and defective high affinity NGF receptor trk-A.

IMR-32 cell line is derived from the neural crest from which the PNS originates. This cell line is known to express only the amplified N-myc but no c-myc gene (Alitalo *et al.*, 1987). This cell line displays several features of orthosympathetic neurons, such as neuron-specific enzymes, receptors and ion channels. For these reasons, this cell line represents a useful model for studying native human nicotinic receptors. The IMR-32 human neuroblastoma cell line expresses both cholinergic and adrenergic neurotransmitter properties. This cell line has previously been used to study the effects of NGF and bFGF (basic fibroblast growth factor) on growth and morphological differentiation (Rabinovsky *et al.*, 1992). Previous studies have also shown that vasoactive intestinal polypeptide (VIP) induces *in vitro* morphological differentiation of the human neuroblastoma lines LA-N-5 and IMR-32 to a degree comparable to that seen with retinoic acid (RA) (Pence and Shorter, 1991). In addition, some studies have shown that neuroblastoma cells such as IMR-32, which over-express N-myc, expressed little or no $\beta 1$, $\alpha 2$, or $\alpha 3$ integrin subunits, as compared with cells which possess only one copy of the N-myc gene (SK-N-SH cells) (Judware and Culp, 1995).

1.10 Diagnosis of Cancer by Fourier Transform Infrared Spectroscopy

Infrared spectra are obtained by passing a beam of polychromatic infrared radiation through a sample and measuring the attenuation of infrared radiation as a function of the wavelength[1]. Infrared or vibrational absorption spectra contain a wealth of information

1. Appendix A describes the principles of FTIR in more detail.

on the molecules: they may be used for the identification and quantification of molecular species, the interactions between neighboring molecules, their state of hydration, their overall shape in the crystalline and in solution phases, and much more. However, its application to tissues has been hampered by problems in sample preparation for optimal spectra acquisition, and most importantly, the strong absorption of IR light by water. By resolving technical and methodological problems, researchers are now able to apply IR spectroscopy to study human tissues (Wong *et al.*, 1991_a; Wong *et al.*, 1993_a).

Neoplastic development is associated with molecular rearrangements or structural changes at the molecular level, altering the vibrational modes of the molecular functional groups in the cells. The changes in the vibrational modes are reflected in the infrared spectrum. Many research groups and individuals are investigating the potential of Fourier Transform Infrared Spectroscopy (FTIR) as a diagnostic tool for the early detection of cancer and also the techniques' ability in detecting biochemical changes associated with the diseased state. In the course of their scientific efforts, it has been established that several changes in the infrared spectra of malignant tissues and cells are common to all cancers including those of colon, stomach, esophagus, skin, liver, cervix and vagina (Wong *et al.*, 1991_b). The primary objective of this thesis is to interpret and investigate the changes in the infrared spectra of IMR-32 cells at the proliferative and differentiation stage induced by cAMP and all *trans* retinoic acid. This could potentially serve as an effective tool to probe the effectiveness of antimitotic drugs.

1.11 Thesis Objectives

The objectives of this thesis are

1) To determine whether the diagnostic bands in the FTIR spectrum accurately reflect the mitotic ability of tumor cells and whether treatment with differentiation inducers introduce spectral changes.

As part of the primary objective, we chose to investigate the effects of all *trans* retinoic acid (tRA) and 8-bromo-adenosine-3':5'-cyclic monophosphate (cAMP) on the *in vitro* growth of a human neuroblastoma cell line (IMR-32). It is also our intention to determine whether the differentiation is advanced enough under these conditions to eliminate the spectral features characteristic of the cells of neoplastic nature.

2) To study the changes in cell morphology and cell growth of treated IMR-32 cells when compared with actively growing cells in order to establish potential relationships with the FTIR spectra.

3) To assess the differentiation progress, we propose to investigate the effect of the two differentiation inducers on the expression and distribution of neurofilament (NF) proteins in the treated IMR-32 cells when compared with actively growing cells.

CHAPTER 2

MATERIALS AND METHODS

2.1 Materials

IMR-32 cells used in this study were obtained from American type culture collection, Rockville, MD, USA. All-*trans* retinoic acid (tRA), mitomycin C, aphidicolin, propidium iodide (PI), and RNAse were purchased from Sigma Chemical Co., St. Louis, MO, USA. 8-bromo-adenosine-3':5'-cyclic monophosphate (cAMP) was purchased from Boehringer Mannheim, Laval, PQ, Canada. Basic fibroblast growth factor (bFGF) was obtained from UBI, Lake Placid, NY, USA. Minimum essential medium (MEM), Dulbecco's phosphate buffered saline (PBS), Trypsin-EDTA and neurobasal medium were purchased from Gibco BRL Life Technologies, Burlington, ON, Canada. Fetal bovine serum (FBS) was obtained from Wisent Inc., St-Bruno, PQ, Canada. Non-essential aminoacids, L-glutamine, sodium pyruvate, nucleosides, penicillin-streptomycin were obtained from Cellgro ^{TM}, Media Tech, Herndon, VA, USA. Bio-Rad reagent for protein assay was purchased from Bio-Rad Laboratories, Richmond, CA, USA. Rabbit anti-neurofilament (200 kDa and 68 kDa) were obtained from Chemicon International Inc, Temecula, CA, USA. Monoclonal anti-neurofilament (70/200 kDa) (mouse) was purchased from ICN Biomedicals, Costa Mesa, CA, USA. Alkaline phosphatase conjugated goat-anti-rabbit-IgG was obtained from Jackson Immuno Research Laboratories, West Grove, PA, USA. Tissue Culture plastic ware (25- and 75-cm^2) flasks and 6-well plates, 100 mm Falcon petri dishes were purchased from Gibco BRL Life Technologies, Burlington, ON, Canada.

2.2 Methods

2.2.1 Cell Culture Maintenance

Human neuroblastoma IMR-32 cells were grown in MEM medium supplemented with 10% fetal bovine serum. These cells were plated at a density of 5 x 10^4 cells/25 cm^2 tissue culture flasks at 37°C in a humidified atmosphere of 95 % air and 5 % CO_2 and sub-cultured twice weekly. The viability of the cells was determined by Trypan blue dye exclusion method.

The cells were harvested from culture flask by trypsinization. Briefly, cells were washed thrice with 5 ml of phosphate-buffered saline (PBS) and incubated with 0.5 ml of trypsin/EDTA for 1-2 min. The detached cells were resuspended in 5 ml of proliferation medium containing FBS and were centrifuged at 1000 rpm for 5 minutes at 4°C.

2.2.2 Cell Treatment

Proliferation Medium. Minimum essential medium (MEM) supplemented with 10% fetal bovine serum, 1% sodium pyruvate, 1% non-essential aminoacids, 1% L-glutamine, 1% nucleosides and 1% penicillin-streptomycin and 0.2% gentamicin.

Proprietary Differentiation Medium and Differentiation Induction. A proprietary medium has been developed and optimized in our laboratory (Dr. J. Phipps, Gap junctions, SIMS, NRC, Canada). The basis is constituted by MEM medium supplemented with 1% sodium pyruvate, 1% non-essential aminoacids, 1% nucleosides, 1% glutamine, 1% penicillin-streptomycin. It also contains neurobasal medium and appropriate supplements.

8-bromo-adenosine-3':5'–cyclic monophosphate (cAMP) (dissolved in PBS) was added to this mixture at a final concentration of 0.5 mM. All-*trans* retinoic acid (tRA) was dissolved in dimethyl sulfoxide (the final concentration of DMSO was less than 0.1%). This concentration of DMSO was not toxic to the cells. The final concentration of tRA was 1 μM in the medium.

Twenty-four hours after plating, the cultures were treated with proprietary differentiation medium containing 0.5 mM cAMP followed by 1 μM all-*trans* retinoic acid treatment the next day. After 5 days of retinoic acid treatment (day 7 of culture), the culture medium was replaced with fresh proprietary differentiation medium containing retinoic acid (1 μM). The culture medium was then changed every 3-4 days, replacing with fresh medium containing the appropriate concentrations of cAMP and retinoic acid. Alterations in morphology and cytotoxicity were assessed microscopically. The cells were photographed using an Olympus microscope equipped with the Image-Pro plus Imaging software after 1, 2, 3, 4, 5 .....20 days.

2.3 FTIR Spectroscopy

IMR-32 cells were trypsinized as described before and the pellet was used for the spectroscopic analysis. Small amounts (about 0.01 mg) of cell samples at room temperature were placed between two KRS-5 (thallium bromide iodide) windows using a glass pipette and then excess water was removed by forced air at room temperature, so that a thin circular deposit of cells was available for recording the spectra. An infrared spectrum at a spectral resolution of 2 cm^{-1} was obtained from each sample at room temperature with a Digilab FTS-40A Fourier transform infrared spectrometer equipped

with a liquid-nitrogen-cooled mercury-cadmium-telluride detector and a KBr beam splitter. For each spectrum, 256 scans were combined and ratioed to a background obtained from a clean KRS-5 window (Rigas and Wong, 1992). Spectra were obtained from samples hydrated in each of water and deuterated water (D_2O). Sample spectra were taken ten minutes after placing the sample holder inside the sample compartment, in order to avoid water vapor interference. In the case of Amide I band study, the cell sample was placed on KRS-5 window, excess water was removed by forced air at room temperature and a drop of D_2O was added on top. The spectra were recorded fifteen minutes after the sample holder was placed inside the compartment. All spectra were converted to absorbance and examined for poor sample preparation, inadequate drying and the presence of artifacts. Data reduction was performed using software developed at National Research Council of Canada, Ottawa, Ontario.

Control Experiments. 1. Cell pellets were obtained as described in Section 2.2.1 and were washed with 0.9% NaCl and recentrifuged to form a pellet again.

2. When PBS was used, the pellet was obtained as follows: after trypsinization, the cells were resuspended in growth medium, washed with PBS and centrifuged again at 1000 rpm for 5 minutes at 4^0 C to form a pellet.

2.4 Cell Cycle Analysis

IMR-32 cells were seeded at a density of 1x 10^5 cells/25 cm^2 tissue culture flask in 5 ml proliferation medium at 37^o C in a humidified atmosphere of 95% air and 5% CO_2.

Forty-eight hours after seeding, individual cultures were treated with aphidicolin (0.6 μg/ml and 1.0 μg/ml), or mitomycin C (10 μg/ ml). After three hours, the mitomycin C treated cells were washed three times with phosphate buffered saline (PBS) and the culture medium was replaced with fresh proliferation medium. After 24 hours treatment, the aphidicolin treated cells were washed with phosphate buffered saline (PBS) and were grown in fresh proliferation medium. The cell enumeration was done with a hematocytometer every 24 hours before and after treatment.

Control as well as treated IMR-32 cells were harvested for cell cycle analysis at 24 and 48 hours after treatment. About $2x10^6$ cells were washed with phosphate buffered saline (PBS) and fixed with 1% paraformaldehyde in PBS for 4 minutes at room temperature. Fixed cells were washed twice with PBS containing 1% bovine serum albumin (PBS-BSA) and permeabilised with absolute methanol (in order to allow propidium iodide to cross the cell membrane) at -20°C for 15 minutes. Permeabilised cells were washed again twice with PBS-BSA and were treated with 5 μg of RNAse/ml in PBS at 37^0C for 20 min (1 ml per million cells). The cells were resuspended in PBS containing 50 μl/ml propidium iodide (PI) (Krishan, 1975). The samples were analysed by flow cytometry (FACS) using a COULTER EPICS Elite ESP (Coulter Corporation, Hialeah, FL, USA). The red fluorescence from PI was measured above 620 nm. PI emission was collected using linear amplification. The final processing of the results was performed by using the multicycle AV software (Phoenix Flow System, San Diego, CA, USA) for DNA content analysis. The levels of DNA per cell allows the discrimination between cells at the G_0/G_1, S and G_2/M phases of the cell cycle. No less than 10,000 cells were analyzed per experiment. The error amounts to 0.08%. This method provides an

analysis of the distribution of the cells among the cell cycle phases, as subpopulations at the G_0/G_1, S and G_2/M phases.

2.5 Immunochemistry

Cell Lysate Preparation. IMR-32 cells were grown in minimum essential medium (MEM) containing 10% fetal bovine serum (FBS) and all additions as stated above. First, the cells were plated at a density of 2.5 x 10^5 cells in 100 mm Falcon petri dishes. Differentiation was induced as described in Section 2.2.2, and the control cells were sampled at day 1 whereas the treated cells were sampled at days 3, 7, 9 and 14 for our experiments.

For cytosolic extraction, the cell cultures were rinsed two times with ice cold phosphate buffered saline (PBS) and were scraped in 600 µl of lysis buffer (10 mM Tris-HCl pH 7.2, 0.16 M Nacl, 1% Triton X-100, 1% sodium deoxycholate, 0.1% sodium dodecyl sulfate (SDS), 1 mM EGTA, 1 mM EDTA, 1 mM phenylmethylsulfonyl fluoride (PMSF), 10 µM leupeptin, 10 µM aprotinin and 100 µM sodium orthovanadate) on ice. The cell lysate was then transferred to a fresh microfuge tube and the DNA was sheared with 21 gauge needle. The cell lysate was then centrifuged at 14000 rpm for 20 minutes at 4°C. The supernatant was treated as whole cell lysate and was used for the immunodetection of neurofilament expression.

Protein concentration was determined with the Bio-Rad protein assay with bovine serum albumin (BSA) as the standard according to the method of Bradford (1976).

Gel Electrophoresis and Western (immuno-) Blotting. Extracts were processed for Western blot analysis in SDS sample buffer (0.625 M Tris-HCl pH 6.8, 2% sodium dodecyl sulfate, 5% mercaptoethanol, 10% glycerol and 0.02% bromophenol blue) and boiled for 3 min at 95°C.

10 μg protein aliquots obtained from each sample as depicted above were resolved by 10% SDS-PAGE (Sodium dodecyl sulfate polyacrylamide gel electrophoresis) according to Laemmli (1970). The resolved proteins were transferred to nitrocellulose membrane (Towbin *et al.*, 1979) in the presence of 25 mM Tris-HCl (pH 8.2), 192 mM glycine, 20% methanol at 100 V for 1 hour. Following transfer, the membranes were incubated for 20 minutes in blocking solution TBST 10 mM Tris (pH 8.0), 150 mM NaCl and 0.05% (v/v) Tween-20 containing 1% (w/v) BSA. A mixture of rabbit polyclonal neurofilament specific antibodies (200 kDa, 68 kDa) and mouse monoclonal anti-neurofilament (70/200 kDa) was added at 1:500 dilution in blocking solution for 1 hour incubation at room temperature. Membranes were washed three times for 5 minutes each in TBS and were then incubated for 1 hour in blocking solution containing 1:5000 diluted alkaline phosphatase conjugated goat-anti-rabbit-IgG (secondary antibody). The membranes were washed three times again with TBS to eliminate the excess antibody and subsequently developed using colored substrate (nitroblue tetrazolium (NBT), 5-bromo-4-chloro-3-indolyl phosphate (BP)).

CHAPTER 3

RESULTS

3.1 Morphological Analysis of IMR-32 Cell Differentiation

In the present study, we used the IMR-32 cell line which was established from highly malignant tumor. The cell line exhibits an amplified N-myc gene and the expression of defective high affinity nerve growth factor receptor trk-A. This cell line is mainly neuroblastic (N-type). Neuronal differentiation was induced by sequential exposure to differentiation inducers such as 0.5 mM 8-bromo-adenosine-3':5'-cyclic monophosphate (cAMP) on day 1 and 1 μM all-*trans* retinoic acid (tRA) on day 2 supplemented in a proprietary medium. These cells were then analyzed for alterations in cell growth and cell morphology. Increased number and length of neuritic processes and pseudoganglia formation were used as markers of IMR-32 cell morphological differentiation. Following 2-3 day exposure of IMR-32 cells to these inducers, the percentage of differentiated cells gradually increased. Figure 3.1 illustrates the appearance of IMR-32 cells at logarithmic phase of growth before treatment with differentiation inducers. Actively proliferating IMR-32 cells at the logarithmic phase (24 h after seeding = day 1) appear primarily as spindle shaped cells (Figure 3.1A). The cytoplasm contains granulations typical of neuro-secretory phenotypes. Occasionally, more flattened fibroblast-like cells are observed. They are, however, not different in molecular terms from the rest of the population. Figure 3.1B illustrates IMR-32 cells at confluent stage. Like with almost every cell line (including cancer cell lines), IMR-32 cells progressively slow down in their growth and finally

Figure 3.1 Phase contrast photomicrographs of IMR-32 cells during proliferation. Cells are grown in the presence of minimum essential medium supplemented with 10% FBS. (A) Actively proliferating IMR-32 cells at the logarithmic phase (24 hrs after seeding=day 1) appear primarily as spindle shaped cells. Here, the DNA is actively synthesized in most cells. Original magnification x 100. (B) IMR-32 cells at confluent stages (day 4). The cells progressively slow down in their growth and finally cease proliferating due to contact inhibition when they reach confluency. Original magnification x 100.


A

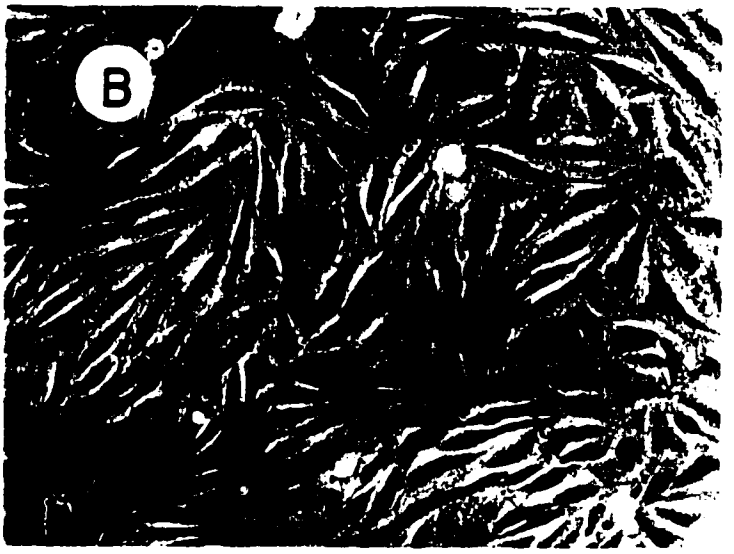
B

cease proliferating due to contact inhibition when they reach confluency. At this stage, they have reached saturation density. The cells remain quiescent for two days and then senesce.

Figure 3.2A illustrates the effect of cAMP on the NB cell line IMR-32. The cells emit neurites. They acquire a rounded morphology and become more birefringent. The combined effect of cAMP and tRA is shown in Figures 3.2B, C, D and E. 1-4 days after treatment with 1 μM tRA (day 3-6), the cells exhibit a variety of shapes from flattened, to spindle, to round. The neurites elongate and thicken. The cells start migrating on the plate. We also found that the two inducers (cAMP+tRA) are potent only when they are provided in combination, otherwise they do not lead the cells to maturation.

At day 7-8 (Figure 3.3A, B) IMR-32 cell bodies gather into dense mounded birefringent clusters forming pseudoganglia. Numerous vesicles form on the neurites. This stage is considered an advanced stage of differentiation. The population is quiescent.

At day 15-20 (Figure 3.4A, B) the cells appeared more differentiated as evidenced by the extension of neurite processes. The pseudoganglia appear as composed of densely packed round birefringent cells sitting on more flattened cells. The pseudoganglia structures remain stable over the following 2-3 weeks until the population senesces. Therefore, IMR-32 cells present a highly morphologically differentiated phenotype under our culture conditions.

The morphological differentiation induced by cAMP and tRA was accompanied by a lower cell proliferation rate than that of the control (Figure 3.5). The growth of treated IMR-32 cells was inhibited when compared to the untreated IMR-32 cells and it correlated with the degree of morphological differentiation. The combination of cAMP

Figure 3.2 Phase contrast photomicrographs of IMR-32 cells after treatment with differentiation inducers. The cells were induced to differentiate in the presence of two inducers, 0.5 mM cAMP on day 1 and 1 μM tRA on day 2 (after seeding) supplemented in a proprietary medium. (A) Upon exposure to 0.5 mM cAMP for 24 h (day 2) the cells emit neurites. (Original magnification x 150) (B) After treatment with 1 μM tRA, the cells exhibit a variety of shapes from flattened, to spindle, to round. The cells have developed a rich neurite network. Treated IMR-32 cells were photographed at various times: (B) on day 3 (original magnification x 150), (C) on day 4, (D) on day 5, (E) on day 6 (Original magnification x 100).

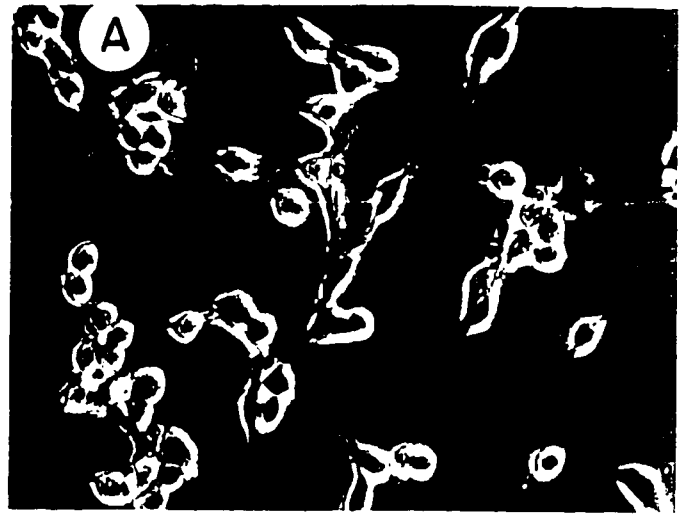
A

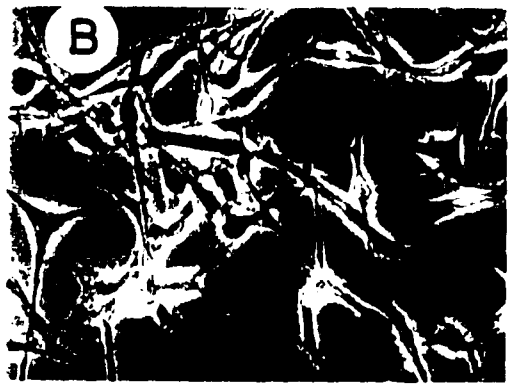
B

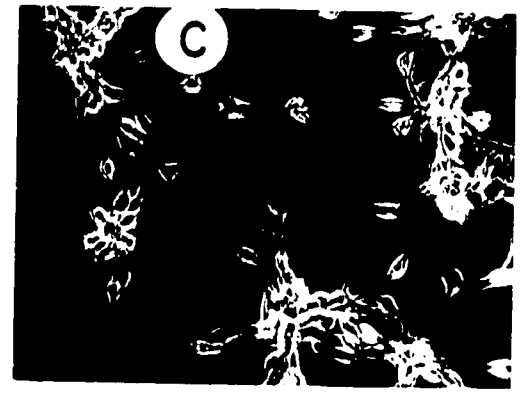
C

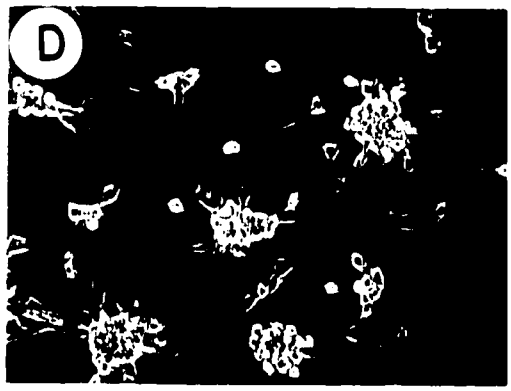
D


E

Figure 3.3 Phase contrast photomicrographs of treated IMR-32 cells. At this stage, the cell bodies gather into dense mounded birefringent clusters forming pseudoganglia. Numerous vesicles form on the neurites. This stage is considered an advanced stage of differentiation. Differentiated cells were photographed at various times: (A) on day 7 and (B) on day 8. (Original magnification x 100)

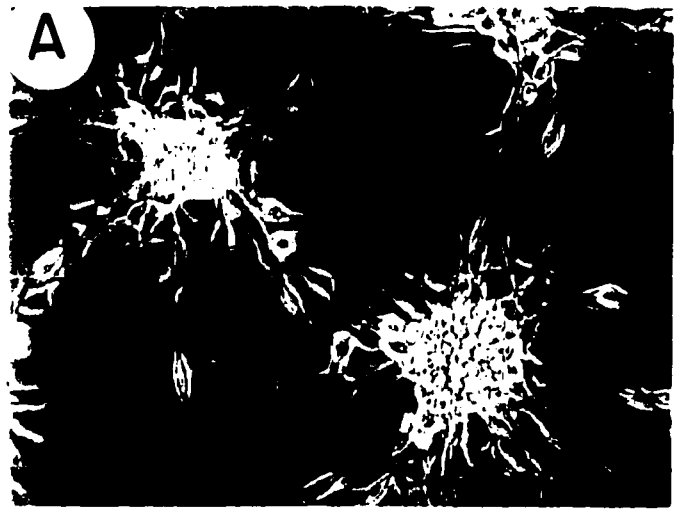
A

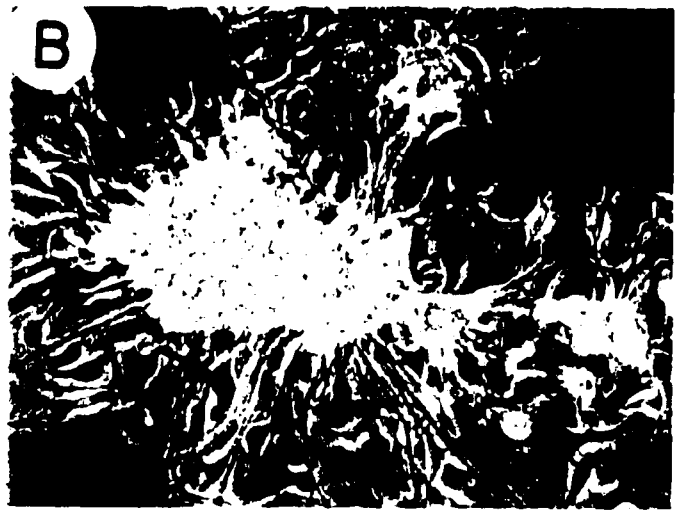
B

Figure 3.4 Phase contrast photomicrographs of IMR-32 cells during differentiation. The pseudoganglia appear as composed of densely packed round birefringent cells sitting on more flattened cells. This ganglion like clusters are associated with an extensive network of neuritic processes. The pseudoganglia structures remain stable over the following 2-3 weeks until the population senesces. Differentiated cells were photographed at various times: (A) On day 15. Original magnification x 100. (B) On day 20. Original magnification x 150.

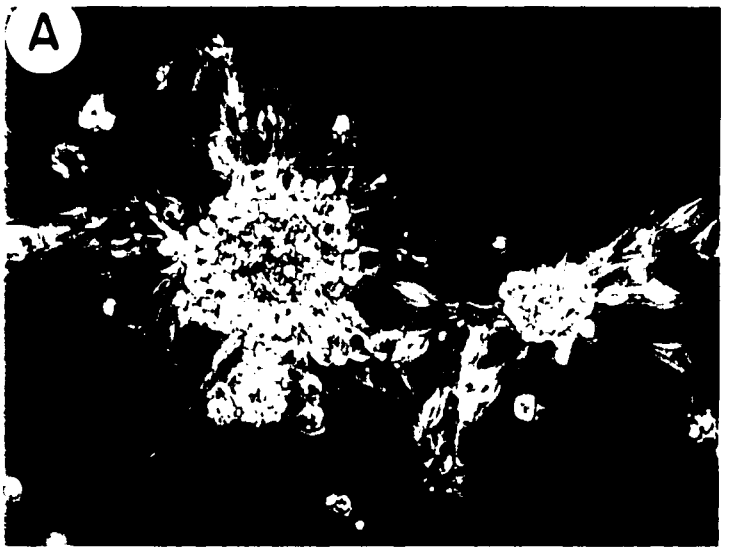
A


B

Figure 3.5 Effect of cAMP and tRA on neuroblastoma cell growth. $1x10^4$ cells per well were seeded in a 6 well tissue culture plate. The cells were harvested and counted using hematocytometer every 24 hours. The green line represents untreated IMR-32 cells. The red line represents IMR-32 cells treated with cAMP and tRA. Data points represent the mean of tripilicate cultures +/- standard deviation.

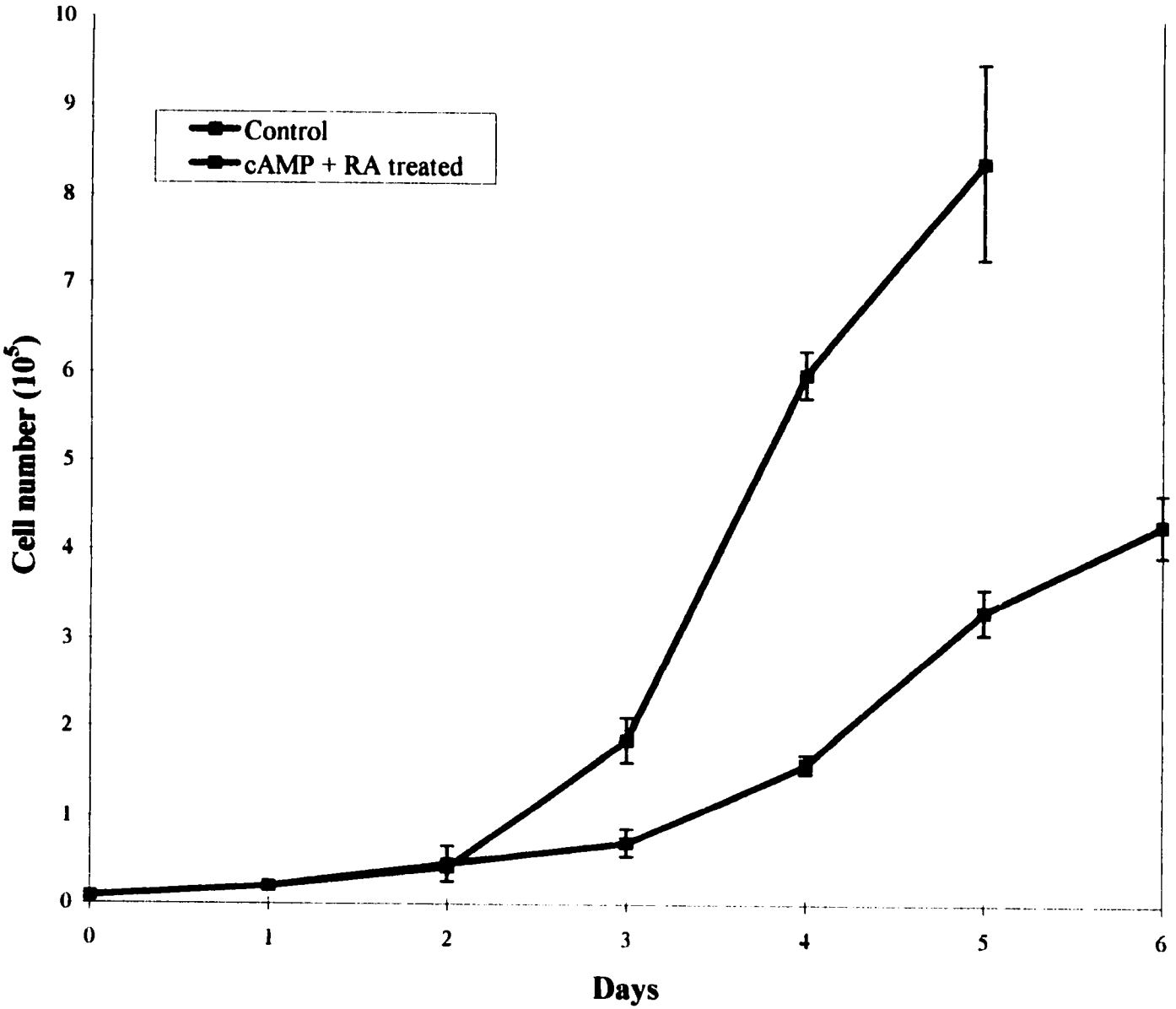
Control
cAMP + RA treated
Cell number (10^5)
Days
0
1
2
3
4
5
6
7
8
9
10

and tRA was found to be very efficient in inhibiting cell growth. Treatment with 0.5 mM cAMP and 1 μM tRA did not exhibit cytotoxic effects because cultures tested at various stages (or days) after treatment are 90% or more viable. We also conducted experiments using varying doses of the tRA inducer, namely: 2.0 μM, 2.5 μM, 5.0 μM, 7.5 μM and 10 μM while keeping the concentration of cAMP constant. We found that for 1 and 2 μM tRA, the concentrations of tRA and cAMP were optimal in inducing morphological and molecular differentiation. Concentrations higher than 2 μM tRA were found to be cytotoxic to the cells. We have used 1 μM tRA with 0.5 mM cAMP throughout our study.

Protein concentrations in homogenate supernatant of both untreated (actively growing) and treated (differentiated) IMR-32 cells were determined with Bio-Rad Protein Assay at each time point from day 1 to day 14 after seeding (shown in Table 3.1). We measured the protein content in each sample in order to apply equal amounts of protein per well. This enabled us to compare the three NF subunit expression on a total protein unit basis.

IMR-32 cells at the mature stage showing highly differentiated morphology were assessed quantitatively in our laboratory (Phipps *et al.*, 1997) and shown to meet the following conventional criteria that define neuronal terminal differentiation: (i) they reach a quiescent stationary phase, (ii) they express markers of mature sympathetic neurons. The evolution of differentiation markers was assessed by flow cytometry analysis (Table 3.2).

Table 3.1

Evolution of the protein content of IMR-32 cells over 14 days [a]

Stage	Protein Content ((μg/ml)of cell lysate)
Actively proliferating (untreated cells)	
Day 1	380
after treatment with cAMP and tRA	
Day 3	540
Day 7	1570
Day 9	1650
Day 11	1650
Day 14	1990
after retro-differentiation[b]	
Day 12	1857

a. The data presented originate from a representative experiment.

b. Treated IMR-32 cells (on day 11) were allowed to undergo retro-differentiation.

Table 3.2

Evolution of specific markers during IMR-32 cells progress into the differentiation program (Phipps *et al.*, 1997).

Stage	Average intensity of emitted fluorescence[a]			
	NSE[b]	CAT[c]	TH[d]	Trk-A[e]
IMR-32 Proliferation (Non-treated)	20.6	92.3	14.4	23.7
+ cAMP (24 hrs after adding cAMP)	20.2	60.1	7.0	38.7
+ cAMP + tRA (3 days after adding cAMP and tRA)	42.6	79.5	25.8	27.2
Mature (7 days after adding cAMP and tRA)	50.3	49.0	85.5	ND
Retro-differentiated[f]	114.4	59.2	27.9	ND

a. The figures are a measure of the average intensity of fluorescence emitted per cell as assessed by FACS analysis. At least 99% of the cells were found to be immunopositive for the markers investigated. The figures provide relative values of the level of expression of the antigen. No less than 10.000 cells were analyzed by flow cytometry. The standard error on the average fluorescence intensity is 0.08%.
b. Neuron specific enolase.
c. Choline acetyl transferase.
d. Tyrosine hydroxylase.
e. High affinity nerve growth factor receptor.
f. On day 11 (the cells were subjected to retro-differentiation on day 9).
ND Not determined.

Neuron specific enolase (NSE) has been regarded as one of the differentiation markers for neuronal cells, but not for glial or Schwann cells in normal neural tissues. It has been shown in previous studies that human neuroblastoma cell line-SH-SY-5Y undergo morphological differentiation and growth inhibition in the presence of TPA or RA and that these changes are accompanied by an increased relative NSE activity, changes which could be expected for differentiating neuroblasts (Pahlman *et al.*, 1984). As previously found, NSE level increases with the progression of differentiation (shown in Table 3.2).

IMR-32 cells express both cholinergic and adrenergic phenotypes. In a previous study with IMR-32 cells, Rabinovsky *et al.* (1992) have demonstrated that CDF (Choline acetyl transferase development factor) treatment increases CAT activity in a dose-dependent manner, independently of cell density. However, CDF does not affect the level of tyrosine hydroxylase (TH) activity, or the rate of cell proliferation. On the other hand, bFGF (basic fibroblast growth factor) induces TH activity and decreases CAT activity in a dose-dependent manner. Its effect on TH is enhanced by increasing cell density, while its reduction of specific CAT activity is independent of cell density (Rabinovsky *et al.*, 1992). As cells differentiate, the level of tyrosine hydroxylase increases whereas the level of CAT decreases. It has been shown that the levels of the two enzymes are inversely correlated (Table 3.2).

This cell line is also known to express defective high affinity NGF receptor trk-A. It has been shown that the majority of primary neuroblastomas express trk-A and at least some of these are able to respond to NGF by inducing terminal differentiation (Azar *et al.*, 1994). The level of trk-A expression was found to be decreased three days after treatment

with differentiation inducers (cAMP and tRA). The trk-A receptor of fully differentiated IMR-32 cells is not functional: the cells do not respond to NGF stimulation (Table 3.2).

Cells are permeable to 8-bromo-cAMP which then causes an increase in intracellular cAMP. This in turn activates the cAMP-dependent protein kinase A (pkA) and related signal transduction pathways whereas RA binds to nuclear receptors that regulate gene transcription and ultimately leads to cellular differentiation.

Previous studies indicate that RA induces the arrest of cell growth in the G1 phase of the cell cycle (Lucarelli *et al.*, 1994). Although both RA and cAMP contribute to the morphological differentiation, these two compounds elicit the transcription of different sets of genes. RA induces a high level of expression of neural genes whereas cAMP induces a chromaffin specific gene pG2 also known as delta like gene in SMS-KCNR cells (Lucarelli *et al.*, 1994).

The morphological differentiation was accompanied by an increase in the expression of neurofilament proteins (another marker of differentiation) as reported for other NB cell lines. The typical neuronal intermediate filament protein, neurofilament (NF) is specific to neurons and neuroblasts and is composed of 3 related polypeptides with molecular weights of 68 kDa, 150 kDa, and 200 kDa (Ross *et al.*, 1988). Studies conducted by Sugimoto *et al.* (1988) showed that immature neurons do not express these proteins (68, 150, 200 kDa). In contrast, differentiated neurons express 68 and 150 kDa proteins and well differentiated neurons express the three protein subtypes.

The expression of neurofilament proteins (68 kDa, 150 kDa and 200 kDa) during differentiation of IMR-32 cells was studied by immunoblot analysis of cell lysates prepared from homogenization of these cells before and after pharmacological treatment.

Equal amounts of total protein of undifferentiated and differentiated cells were assayed for immunoreactivity of this intermediate filament protein using monoclonal and polyclonal antibodies that recognize specifically each protein.

Untreated (actively growing stage) and treated (differentiating stages) IMR-32 cells were harvested at various times: control on day 1, treated on day 3, 7, 9, 11, 14 for our analysis. Figure 3.6 shows immunoblots of IMR-32 extracts before and after treatment. The levels of expression of neurofilament protein evolves with the progress of differentiation.

Mitotically active IMR-32 cells show the presence of a light phosphorylated form of the 150 kDa NF subunit. Treated IMR-32 cells on day 3 exhibit similar phosphorylated form of 150 kDa subunit whereas the intensity of 150 kDa subunit is higher on day 3 compared to untreated cells. Both control and treated IMR-32 cells on day 3 after differentiation induction indicate a lack of expression of the 68 and 200 kDa NF subunits. From day 7 - day 14, we observe a gradual increase in the intensity of the phosphorylated form of 68 kDa NF subunit as well as an increase in the intensity of the phosphorylated form of 200 kDa subunit of neurofilament. On the other hand, the single band of the 150 kDa subunit of neurofilament appears to be weak on day 7 and day 9 but it increases steadily in intensity from day 11 to 14. The appearance of these three bands and their different level of expression are associated with the morphological changes shown in Section 3.1. We found that in treated IMR-32 cells the acquisition of a mature neuronal phenotype is accompanied by an increase in the expression of neurofilament proteins.

Figure 3.6 Western-blotting analysis of the expression of neurofilament triplet protein in IMR-32 cells during differentiation. Cell extracts, prepared using lysis buffer, were analyzed as described in Section 2.5, with equal amounts of protein applied for each sample. Samples shown are (1) Untreated IMR-32 cells. Treated IMR-32 cells were harvested at various times (2) Day 3 (3) Day 7 (4) Day 9 (5) Day 11 (6) Day 14 for our experiment. Lane 7 represents retro-differentiated IMR-32 cells harvested on day 12 (Refer to page 57 for more details).

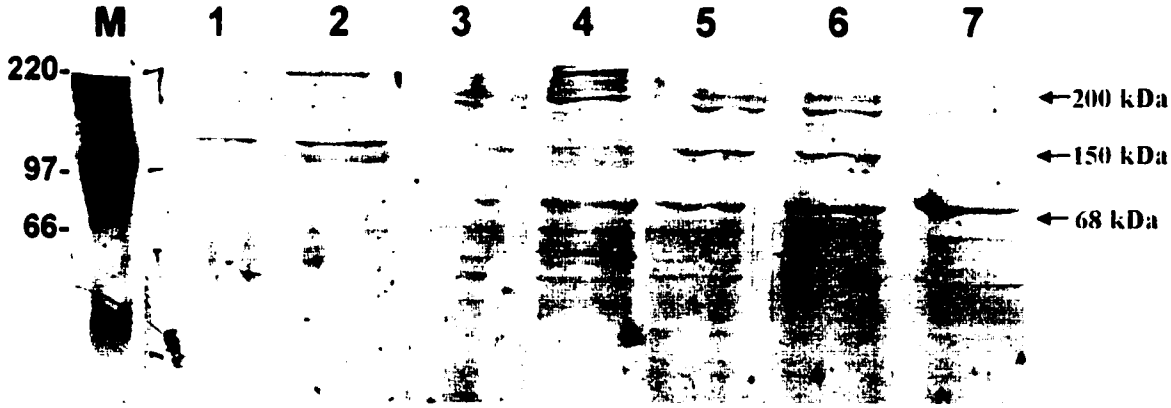
M
1
2
3
4
5
6
7
220-
97-
66-
←200 kDa
←150 kDa
← 68 kDa

3.2 Spectroscopic Analysis of IMR-32 Cell Differentiation

The assignments of infrared bands in biological tissues and cells has been well established in the literature by studying the infrared spectra of isolated DNA, RNA, nuclei, skeletal proteins, membrane lipids and other biomolecules from tissues and cells (Wong *et al.*, 1995). A reference Table 1 in Appendix B summarizes the characteristic bands for proteins, lipids, nucleic acids and carbohydrates in the infrared spectra of the cervical tissues and cells (Wong *et al.*, 1995).

Figure 3.7 represents the infrared spectrum obtained for untreated (actively growing) IMR-32 cells in the frequency region 950 to 1500 cm^{-1}. The band peaking at 970 cm^{-1} in the figure is due to the symmetric stretching mode of dianionic phosphate monoesters of phosphorylated proteins and cellular nucleic acids. Previous studies have suggested that the presence of this band might serve as a key indicator for malignancy (Wong *et al.*, 1991_a). However, this band is present in both untreated and treated IMR-32 cells (data not shown).

3.2.1 Vibration of $-CH_2OH$ and C-OH Groups of Carbohydrates

Three other significant bands observed in my experiments are discussed with reference to Figure 3.8 which illustrates the representative infrared spectra of untreated (actively growing) and treated (differentiated) IMR-32 cells in the frequency region 1000-1350 cm^{-1}. The shape and peak positions of all the infrared bands in these three spectra are almost the same.

Figure 3.7 Infrared spectrum of IMR-32 cells at the actively growing stage in the frequency region 950 to 1500 cm^{-1}.

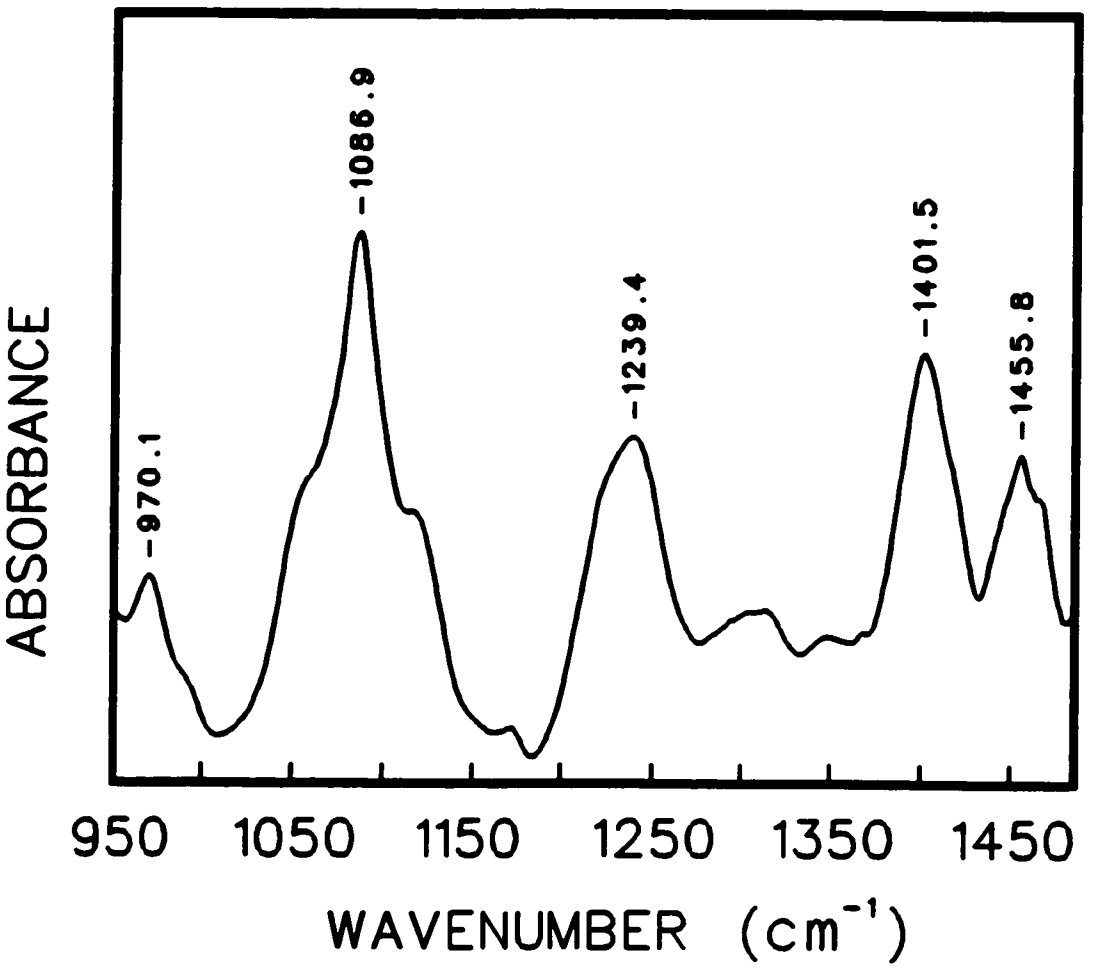
ABSORBANCE
970.1
1086.9
1239.4
1401.5
1455.8
950
1050
1150
1250
1350
1450
WAVENUMBER (cm⁻¹)

Figure 3.8 Phosphate stretching region of the infrared spectrum of IMR-32 cells before (solid line) and after treatment with differentiation inducers (cAMP and tRA) for a period of 7 days (short dash line) or 14 days (long dash line).

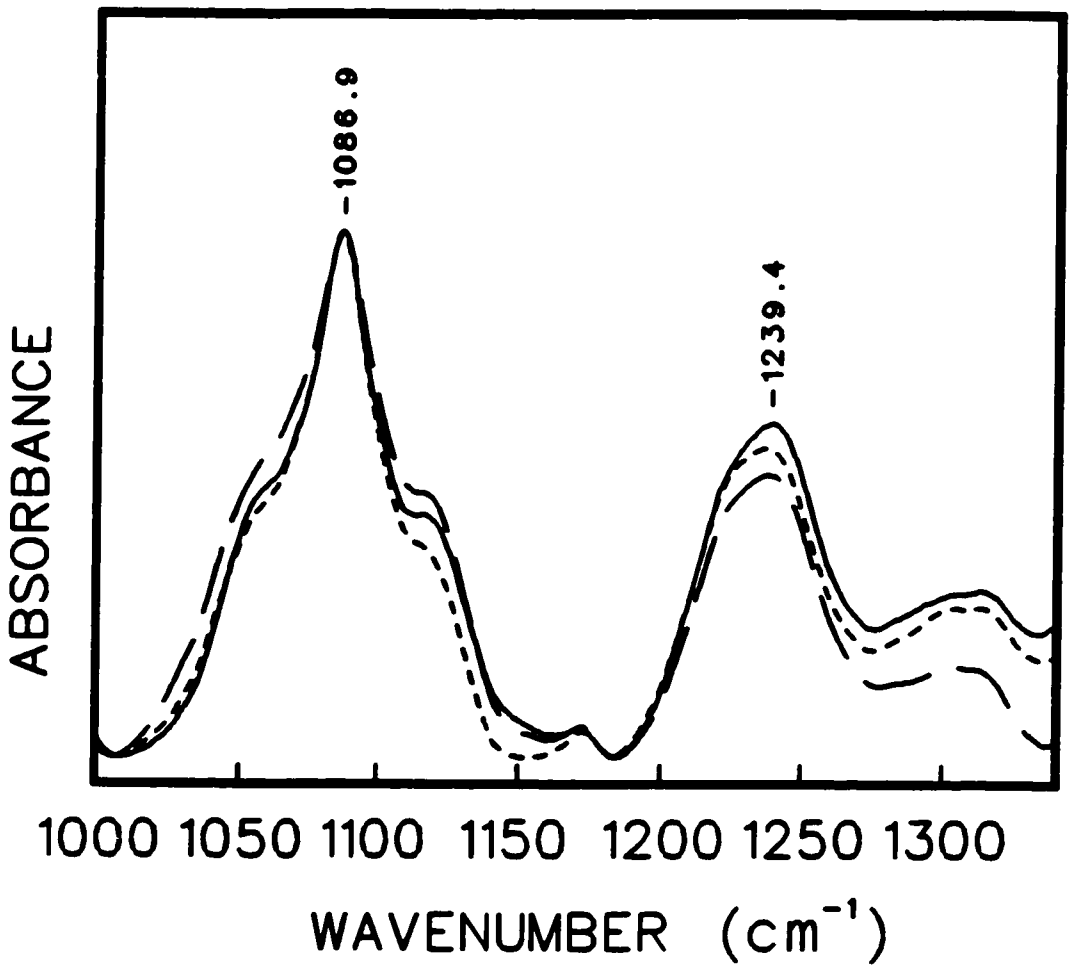
1086.9
1239.4
ABSORBANCE
1000 1050 1100 1150 1200 1250 1300
WAVENUMBER (cm⁻¹)

Several overlapping bands in the frequency region of 1000 to 1080 cm^{-1}, such as the bands of 1031 cm^{-1} and 1055 cm^{-1}, are mainly due to the vibrational mode of the -CH_2OH groups and the C-O stretching coupled with C-O bending of the C-OH groups of carbohydrates. The presence of the 1031 cm^{-1} band is ascertained and its frequency is obtained from third-power-derivative spectra with the use of a breakpoint of 0.3 in the Fourier domain by software developed in NRCC laboratory (Kauppinen *et al.*, 1981).

Earlier studies have shown that the infrared spectrum of D-glycogen from mammalian liver is essentially superimposable with this band in the frequency region 975-1080 cm^{-1} (Wong *et al.*, 1991_c). Significant changes in the intensity of the glycogen bands in the frequency region 1000-1060 cm^{-1} were observed between normal and malignant samples. The authors have shown that the amount of glycogen dramatically decreased in exfoliated cells from cancerous cervical tissue compared with those from normal cervical tissue.

However, the IR spectrum obtained in this study as shown in Figure 3.8 exhibits no significant changes in the intensity of the glycogen bands in the frequency region 1000-1060 cm^{-1} between untreated and treated IMR-32 samples.

3.2.2 Symmetric and Asymmetric Phosphate Stretching Region

A significant number of striking changes in the spectra common to various malignant tissues and cells lie in the symmetric ($\nu_s PO_2^-$) and asymmetric ($\nu_{as} PO_2^-$) stretching modes of phosphodiester groups. These changes are applicable to malignant tissues and cells common to cancers of colon, stomach, esophagus, cervix and vagina (Wong *et al.*, 1991_b).

The band at 1082 cm^{-1} is due mainly to the symmetric phosphate stretching mode. The band at 1244 cm^{-1} is due to the asymmetric phosphate stretching mode. Though it is well known that phosphate groups are present in both nucleic acids and phospholipids, studies conducted with cultured human adenocarcinoma colon cells and malignant colon tissue by Wong *et al.* (1991_b) have shown that the vibrations from phosphate groups originate mainly in the phosphodiester groups of nucleic acids. This has been accomplished by taking the peak intensity ratio between the C=O stretching band of the carbonyl group of lipids at 1740 cm^{-1} and the asymmetric phosphate stretching band at 1240 cm^{-1}. The results obtained from these studies show that phosphate groups of phospholipids contribute minimally to these bands. The amount of other compounds containing phosphodiester groups in tissues and cells is much smaller than that of phospholipids. Therefore their contribution to the intensities of these phosphate stretching bands in the infrared spectra of tissue and cells is also negligible (Wong *et al.*, 1991_b).

The amide III band could theoretically contribute to the intensity of the asymmetric phosphate stretching band at 1244 cm^{-1}. However, its frequency varies according to the secondary structure of proteins. The secondary structure of proteins can be determined by the frequency of the amide I band. The peak position of the amide I band of proteins in both treated (differentiated) and untreated (actively growing) IMR-32 cells is at 1652 cm^{-1} (with reference to the original spectra) which indicates that the secondary structure of the proteins in both samples is mainly α-helical (data not shown). The amide III band of proteins with α-helical structure is located in the frequency region 1260-1290 cm^{-1} which is much higher than the frequency of the asymmetric phosphate stretching band

(Wong *et al.*, 1991_c) and therefore, it does not contribute to the intensity of the 1244 cm^{-1} band in the spectra of treated and untreated IMR-32 cells.

Significant changes in the intensity of the symmetrical phosphate stretching band as well as shift in the peak position are commonly observed between the spectra of normal and cancer cells. The symmetrical phosphate stretching band in normal tissue or cells peaks at 1082 cm^{-1}, whereas in malignant tissue or cells, this peak is shifted to 1086 cm^{-1} (Rigas *et al.*, 1990). This phenomenon indicates that the intermolecular interactions among nucleic acids in the malignant tissue or cells are stronger as a result of a tighter intermolecular packing. This has also been observed in other cancerous tissues and cells (Wong *et al.*, 1993_a).

The results obtained from the present study as shown in Figure 3.8 indicate **neither frequency shift nor change in band shape** in the symmetrical phosphate stretching band between untreated (actively growing stage) and treated (differentiated) IMR-32 cells. The frequency observed at this region ranges from 1086 to 1087 cm^{-1} for both samples and is found to be reproducible throughout the study.

The asymmetric phosphate stretching band is usually broad and consists of two overlapping bands with the maxima near 1220 and 1240 cm^{-1} for cancer cells. In contrast, the spectrum of normal cells has no detectable 1220 cm^{-1} band, while a narrow band peaking at or above 1240 cm^{-1} is observed (Rigas *et al.*, 1990). The frequency of the asymmetric phosphate stretching band is at ~1220 cm^{-1} when the phosphate group is fully hydrogen bonded and at or above 1240 cm^{-1} when it is not hydrogen bonded. The results obtained from the earlier study show the low frequency component band in the malignant tissue or cells is markedly increased in intensity when compared with that of normal tissue

or cells. They also concluded that a large number of phosphodiester groups of nucleic acids are hydrogen bonded in the case of malignant cells. However, the results obtained in this thesis work as shown in Figure 3.9 indicate the presence of these two component bands in both the spectra of untreated (actively growing stage) and treated (differentiated) IMR-32 cells. Figure 3.9 shows increase in relative intensity of the low frequency component band of treated IMR-32 cells. This indicates that the number of hydrated phosphate groups has increased in the nucleic acids of the treated IMR-32 cells.

Thus IMR-32 cells at actively growing stage (logarithmic phase) and the differentiated IMR-32 cells exhibit quite similar spectral characteristics in the symmetric and asymmetric phosphate stretching region. **In spite of IMR-32 cells meeting the criteria associated with terminal differentiation (quiescence, high level of morphological and molecular differentiation) their malignant nature is perceived by spectroscopic results.** Normally one would expect that terminally differentiated neurons exit the cell cycle and die when challenged to grow. But differentiated IMR-32 cells in our case undergo reproliferation as explained in section 3.3.

3.2.3 Amide I Band

There are many vibrational bands characteristic of peptide groups and side chains from which information on protein structures can be obtained. Among these, the amide I band between 1600-1700 cm^{-1} is specially sensitive to the secondary structure of proteins (Torii and Tasumi, 1996).

The amide I band arises from C=O (80%) stretching vibrations weakly coupled to C-N stretching vibrations (20%). The amide II band (1545 cm^{-1}), on the other hand,

Figure 3.9 Deconvolved infrared spectrum of IMR-32 cells in the asymmetric phosphate stretching region. Untreated IMR-32 cells (actively growing stage) is shown by (solid line) and treated IMR-32 cells (with cAMP and tRA) for a period of 7 days (short dash line) or 14 days (long dash line). Spectra were Fourier self-deconvolved with a resolution enhancement factor of 1.5 and a bandwidth of 17 cm^{-1}.

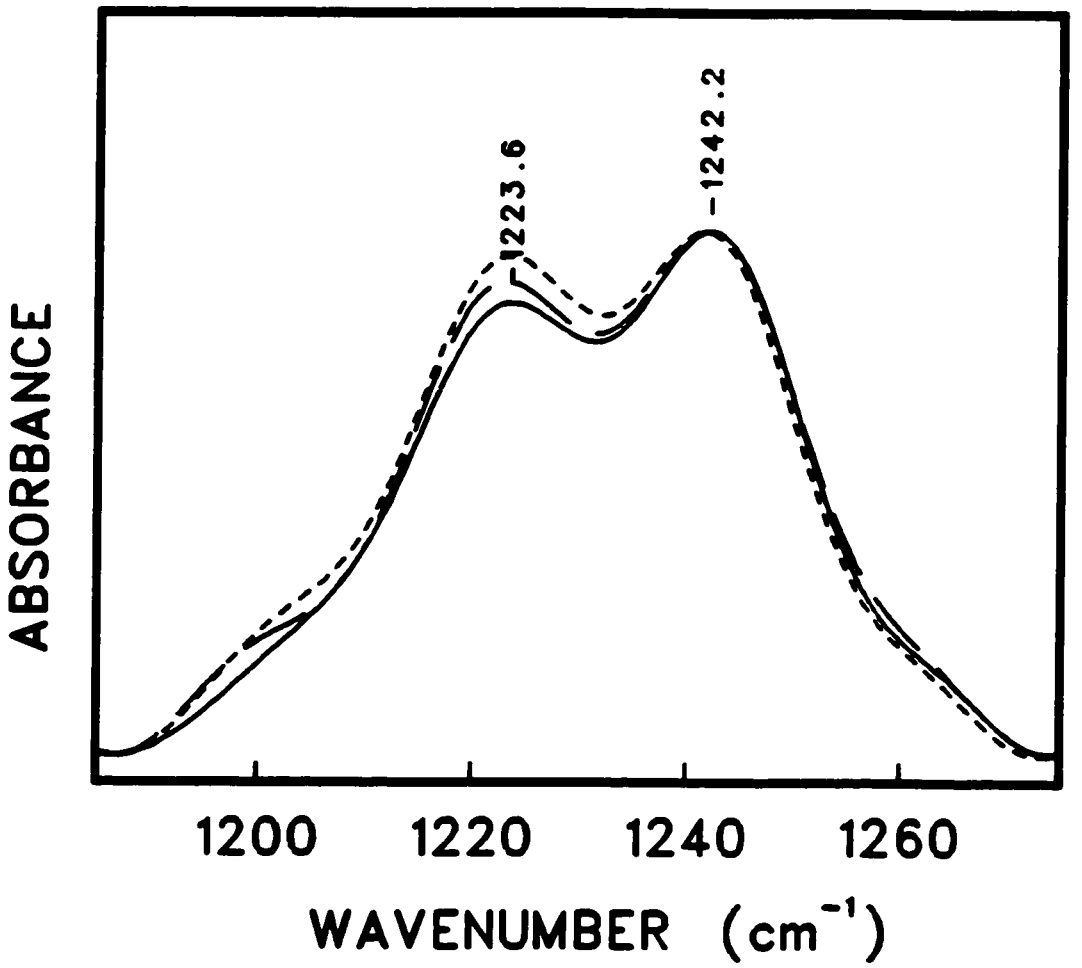
1223.6
1242.2
ABSORBANCE
1200
1220
1240
1260
WAVENUMBER (cm^{-1})

arises from N-H bending vibrations (60%) coupled to C-N stretching vibrations (40%). Sensitivity of the amide II band to polypeptide backbone conformation is not well established. The amide III band, although sensitive to secondary structure, gives rise to a weak IR band. The exact frequency of the amide I band depends on the nature of H-bonding involving the CO and NH groups and on the geometry of the molecule. This in turn depends on the secondary structure adopted by the protein.

The conformation sensitive amide I band is a composite band consisting of overlapping component bands originating from different structures such as α-helices, β-strands, turns and unordered polypeptide fragments. Resolution enhancement techniques allow us to identify the component bands and determine the proportion of various conformers.

The peak maximum of the amide I band is sensitive to the secondary structure in proteins. The α-helical structure has its peak maximum near 1653 cm^{-1}, the parallel β-sheet near 1635 cm^{-1}, the antiparallel β–sheet near 1637, 1683 cm^{-1} and β-turn between 1660 to 1690 cm^{-1}. The amide I bands of unordered random coils and turns are at around 1645 cm^{-1} and 1665 cm^{-1}, respectively. A band near 1612 cm^{-1} is due to the amide I mode of the amide groups in which the hydrogen bonds are formed between neighboring protein molecules (Wong *et al.*, 1993_b). Previous studies have shown that the position of the major component band at 1612 cm^{-1} is somewhat below the frequency range typical for β-sheets in globular proteins (Susi and Byler, 1986). Hence the presence of band near 1612 cm^{-1} in our results may reflect the formation of an intermolecularly hydrogen-bonded β-sheet structure. Furthermore, the intensity of this band is a measure of the magnitude of intermolecular aggregation in proteins. Since each globular protein

molecule contains segments with different substructures, the amide I band of globular proteins usually appears as a broad band with several maxima. The changes in the relative intensities of these maxima can be used to monitor changes in the secondary substructures of globular proteins (Wong *et al.*, 1993_b).

The results shown in Figure 3.10 compares the enlarged amide I band spectra of the entire population of cellular proteins in the untreated (actively growing stage) and the treated (differentiated) IMR-32 cells. Figure 3.10A shows the original spectra and the corresponding deconvolved spectra is shown in Figure 3.10B. The figure indicates that the cellular proteins are to a large extent α-helices with considerable segments of β-sheet. Furthermore, the spectra revealed the presence of an additional band near 1612 cm^{-1} due to intermolecular amide groups.

Differentiated IMR-32 cells exhibit changes in the amide I band region of the spectrum, when compared to their untreated controls. The decrease in the intensity of the 1612 cm^{-1} band in differentiated IMR-32 cells indicates the reduction of the inter-molecular hydrogen-bond aggregation between neighboring protein molecules (dissociation of protein aggregates) during differentiation (Figure 3.10).

The above mentioned spectral results of IMR-32 cell is different from the observations of Wong *et al.* (1993_a) on human colonic tissues. When the authors studied normal and malignant colonic tissues in the amide I band region, they found that the relative intensity of the 1612 cm^{-1} band in the malignant tissue decreases when compared to the normal tissue.

Figure 3.10 Infrared spectrum of IMR-32 cells in the amide I band region before (solid line) and after (short dash line) treatment with differentiation inducers (cAMP and tRA) for a period of 7 days. (A) Original spectra. (B) Corresponding deconvolved spectra with an enhancement factor of 1.5 and a bandwidth of 17 cm^{-1}.

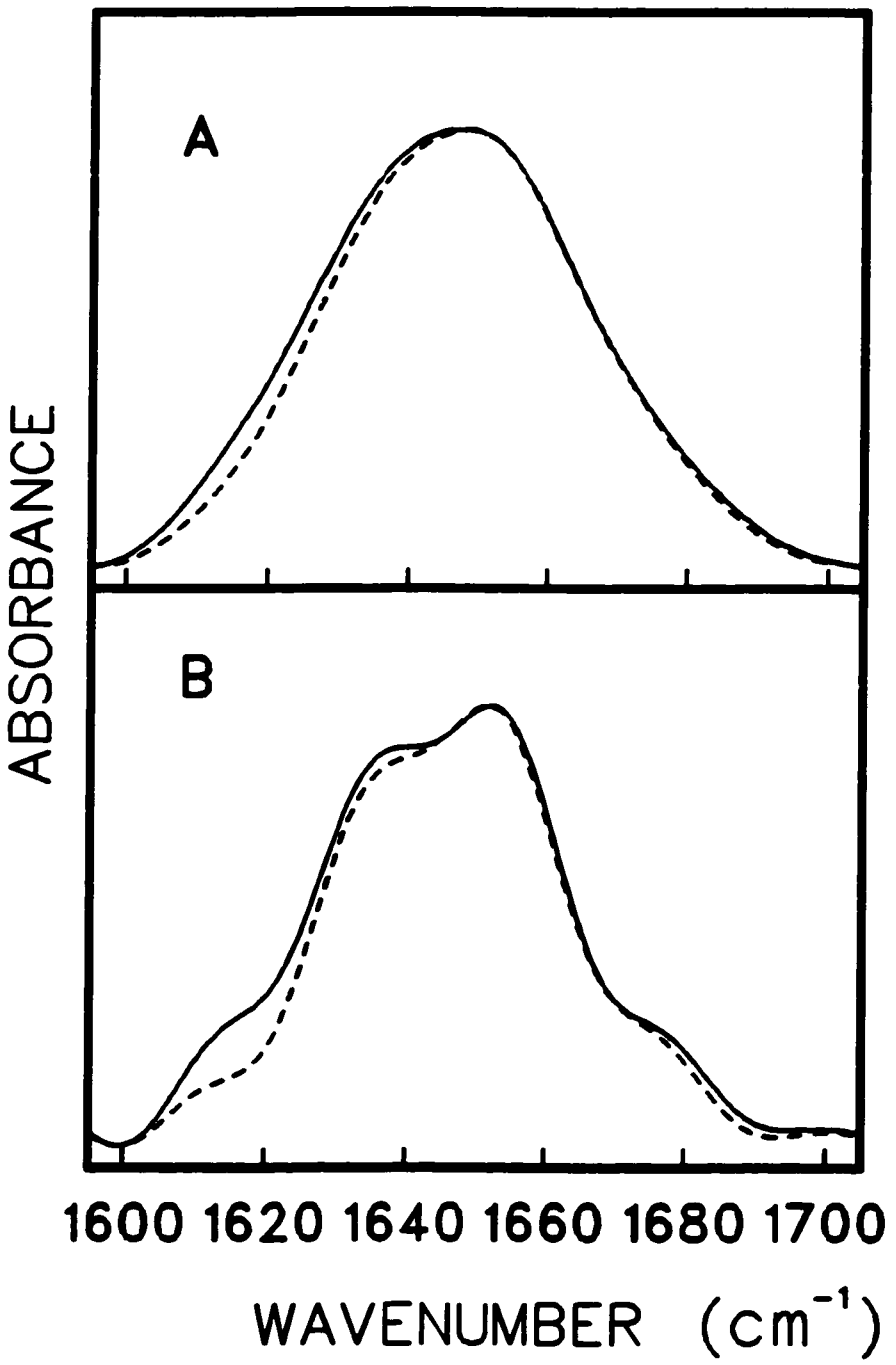
A
B
ABSORBANCE
1600 1620 1640 1660 1680 1700
WAVENUMBER (cm^{-1})

3.2.4 Summary of Spectral Analysis

When compared with controls, the IMR-32 cells treated with cAMP and tRA exhibit the following changes:

1) a band peaking at 970 cm^{-1} in spite of treatment,

2) no significant changes in the intensity of the glycogen bands,

3) no changes in the symmetric and asymmetric phosphate stretching region,

4) changes in the amide I band region of the spectrum.

The observation 1) pertaining to IMR-32 cells implies that despite a high level of molecular and morphological differentiation, the malignant nature of the cells is still perceived by the test. However changes in the amide I band region reflect the drastic cytosolic molecular modifications due to differentiation.

3.3 Retro-Differentiation of IMR-32 cells

The results shown in Section 3.2 indicate no spectral changes at the symmetric and asymmetric phosphate stretching band of the phosphodiester groups of nucleic acid after treatment with cAMP and tRA. The spectral results further imply that IMR-32 cells may have retained the potential to proliferate again to original cancer cells under appropriate conditions, despite reaching a fully differentiated stage as assessed by several conventional criteria. This hypothesis was tested by challenging the differentiated cells to resume proliferation. This method involved trypsinizing the differentiated IMR-32 cells and allowing them to grow in the presence of the proliferation medium.

Cells resumed proliferation at the same rate as their controls (actively growing stage). Simultaneously the cells retracted their neurites and the final morphological structure

looked similar to that of the original cancer cells (Figure 3.11A and B): the cells retro-differentiate. Even at more advanced stages of differentiation (fully mature), IMR-32 cells (at 15-20 days) undergo reproliferation (within 24 hours) when challenged to grow. It was found that these differentiated cells also undergo retro-differentiation since they retract their neurites and acquire a neuroblast morphology. The level of the differentiation markers tends to return to those indicative of the mitotic phenotype.

The spectral results indicated that retro-differentiated IMR-32 cells exhibit no changes in the symmetrical and asymmetrical phosphate stretching region when compared to the actively proliferating IMR-32 cells (Figure 3.12 and Figure 3.13) and the amide I band returns to the spectrum shown by actively proliferating IMR-32 cells (Figure 3.14). Despite the changes in the intensity of the band at 1612 cm^{-1} in differentiated IMR-32 cells, retro-differentiated IMR-32 cells exhibit the same spectral characteristics as that of original cancer cells especially in the amide I band region.

Total cellular protein levels of retro-differentiated IMR-32 cells (Day 12) per ml of cell lysate was determined with Bio-Rad Protein Assay and is shown in Table 3.1.

Western-blotting analysis was conducted on the retro-differentiated IMR-32 cells. Compared to differentiated IMR-32 cells (on day 14), retro-differentiated IMR-32 cells lacked the 150 kDa subunit of neurofilament and showed decrease in the intensity of 200 kDa band. However, no change in the intensity of the phosphorylated form of 68 kDa band was observed when compared to the differentiated IMR-32 cells (Figure 3.6).

The evolution of differentiation markers such as neuron-specific enolase, tyrosine hydroxylase, choline acetyl transferase and the expression of high affinity nerve growth

Figure 3.11 Phase contrast photomicrographs of retro-differentiated IMR-32 cells. Upon removal of the inducers and transfer into 10%FBS MEM based medium, differentiated IMR-32 cells readily retract their neurites and proliferate at the same rate as the controls. This photomicrograph shows retro-differentiated IMR-32 cells after sub-culture.

(A) Retro-differentiated IMR-32 cells. Original magnification x 100.
(Differentiated IMR-32 cells are subjected to retro-differentiation on day 7 and the retro-differentiated IMR-32 cells are photographed on day 8).

(B) Actively growing IMR-32 cells. Original magnification x 100.


A


B

Figure 3.12 Phosphate stretching region of the infrared spectrum of IMR-32 cells at actively growing stage (solid line) and after treatment with differentiation inducers (cAMP and tRA) for a period of 6 days and retro-differentiation through transfer into growth medium (short dash line).

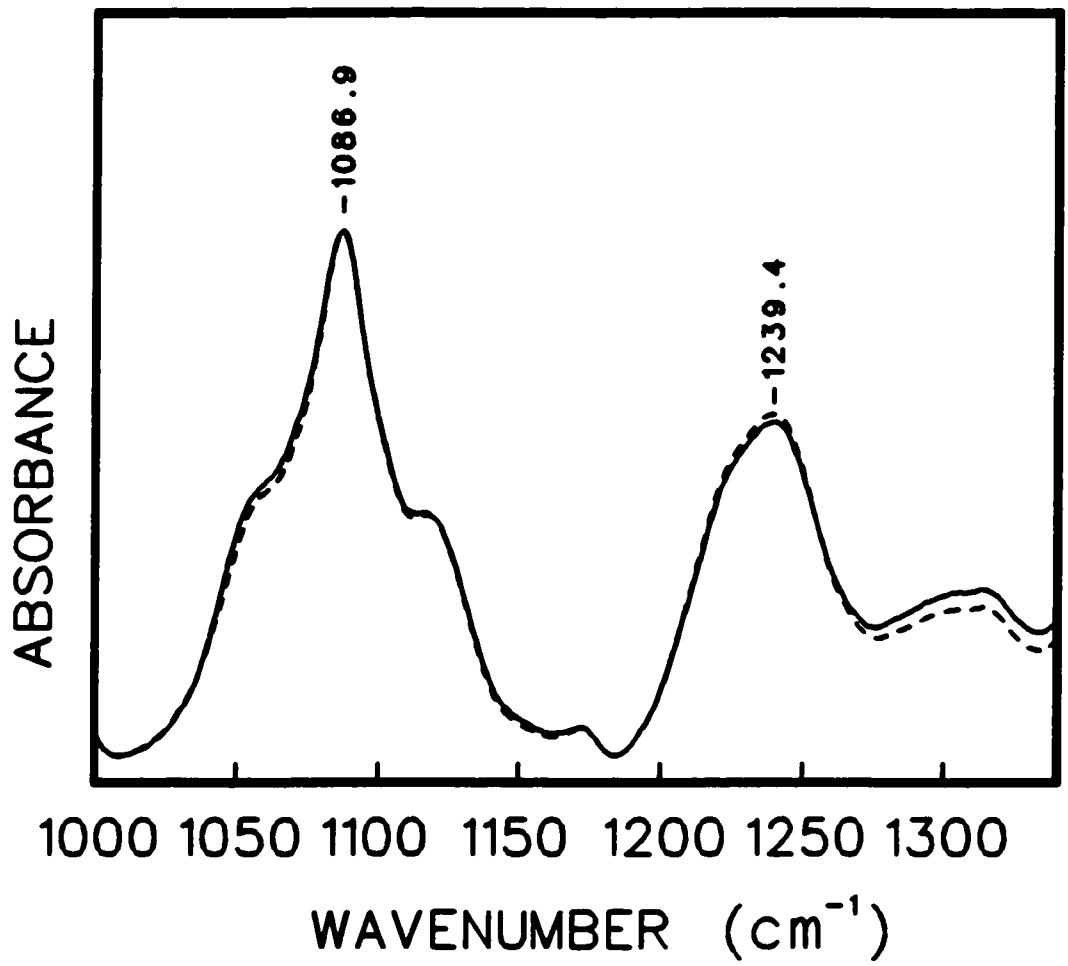
1086.9
1239.4
ABSORBANCE
1000 1050 1100 1150 1200 1250 1300
WAVENUMBER (cm^{-1})

Figure 3.13 Deconvolved infrared spectrum of IMR-32 cells in the asymmetric phosphate stretching region. Solid line represents deconvolved spectrum of untreated cells (actively growing stage) and the short dash line represents treated IMR-32 cells (with cAMP and tRA) for a period of 6 days and retro-differentiation through transfer into growth medium. Spectra were Fourier self-deconvolved with an enhancement factor of 1.5 and a bandwidth of 17 cm^{-1}.

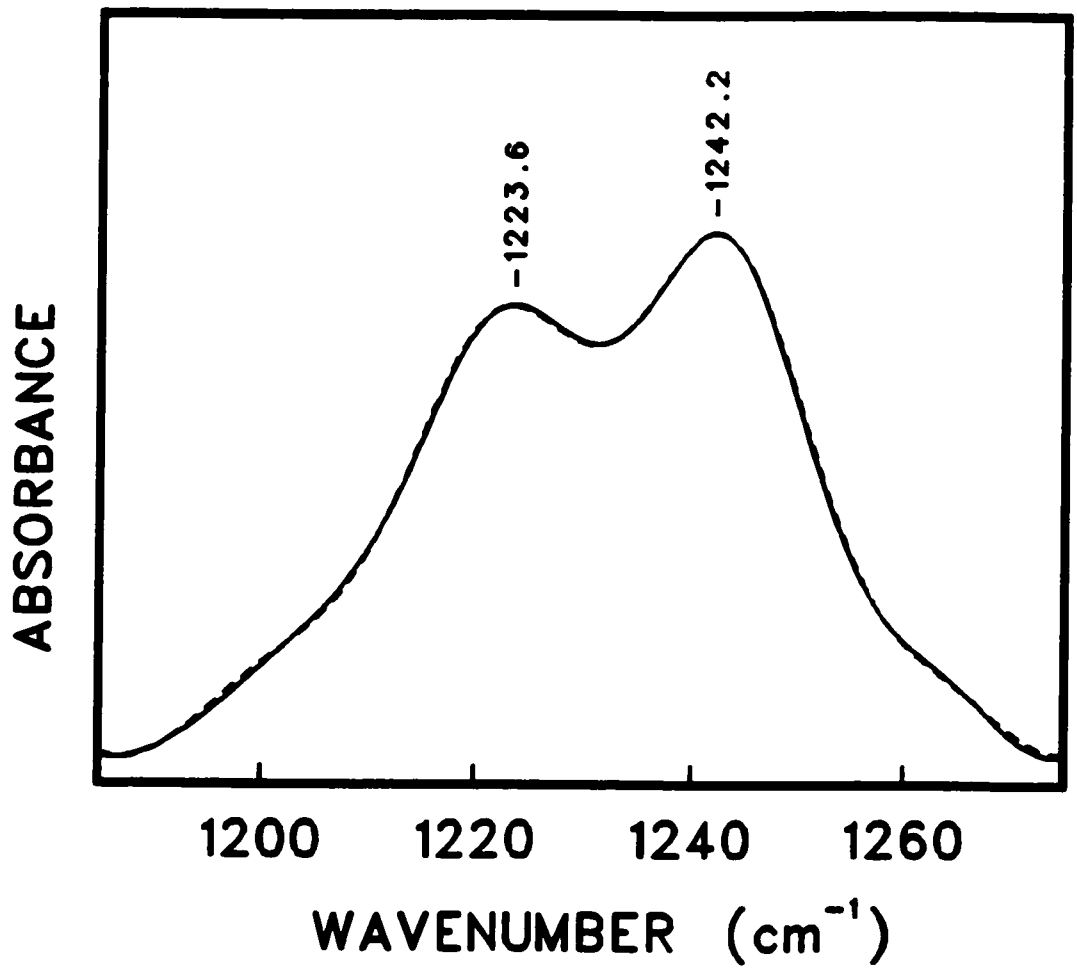
ABSORBANCE
1223.6
1242.2
1200
1220
1240
1260
WAVENUMBER (cm^{-1})

Figure 3.14 Amide I band region of the deconvolved infrared spectrum of IMR-32 cells at actively growing stage (solid line) and after treatment with differentiation inducers (cAMP and tRA) for a period of 6 days and retro-differentiation through transfer into growth medium (short dash line). Spectra were Fourier self-deconvolved with an enhancement factor of 1.5 and a bandwidth of 17 cm^{-1}.

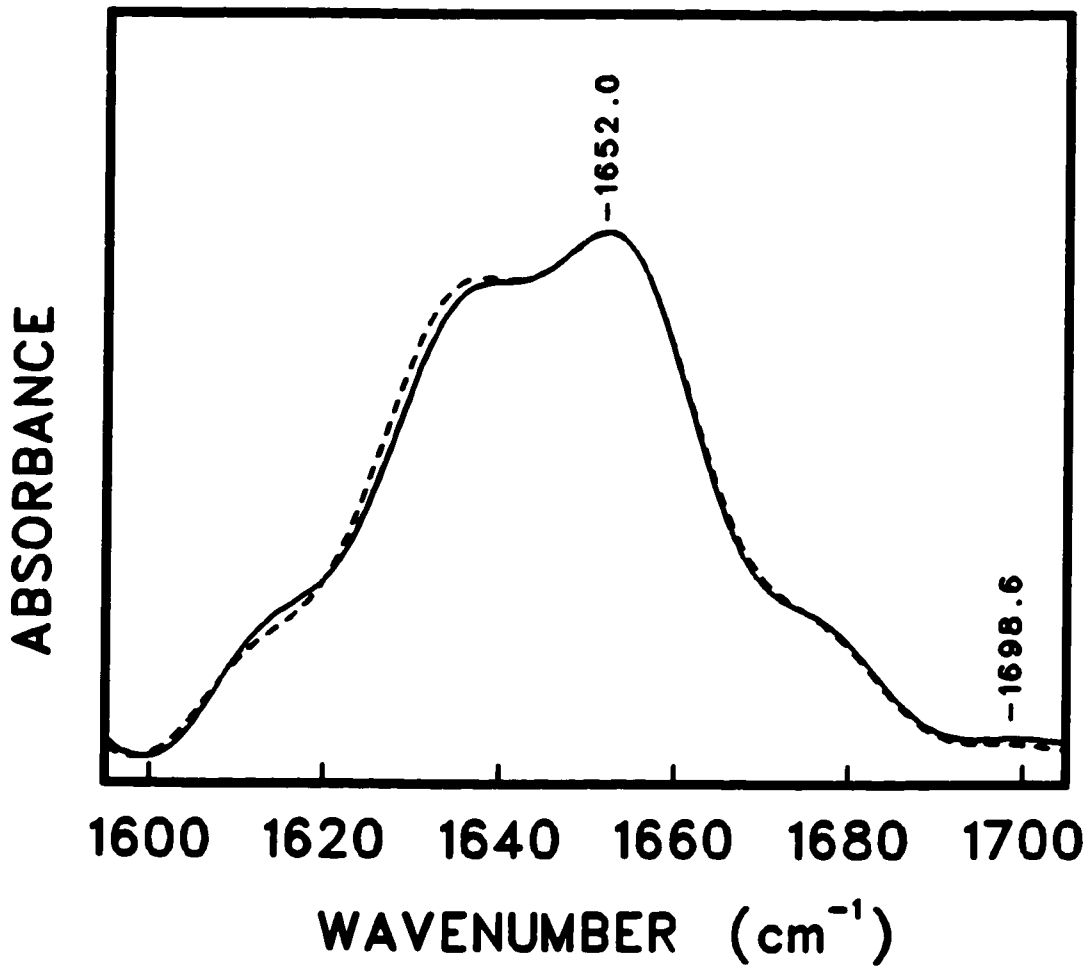
1652.0
1698.6
ABSORBANCE
1600
1620
1640
1660
1680
1700
WAVENUMBER (cm^{-1})

factor receptor trk-A (shown in Table 3.2) were assessed by flow cytometry analysis for the retro-differentiated IMR-32 cells in our laboratory (Phipps *et al.*, 1997).

It was found that

(1) the level of NSE in retro-differentiated IMR-32 cells is higher than in actively growing IMR-32 cells. This is because the retro-differentiated cells have reached confluent stage after two days.

(2) the level of CAT in retro-differentiated IMR-32 cells is lower than in actively growing IMR-32 cells but a tendency to increase after two days is observed.

(3) the level of TH in retro-differentiated IMR-32 cells is higher than in actively growing cells though it is decreasing rapidly.

Thus there is a general trend of differentiation marker levels in retro-differentiated IMR-32 cells returning to the values observed in growing cells.

The overall conclusion is that the differentiation inducers (cAMP and tRA) used in this study are effective in controlling growth of IMR-32 cells but they have to be present in the medium to maintain growth inhibition. The cells have not reached the terminal differentiation stage associated with terminal exit from the cell cycle.

3.4 Effect of Cell Cycle Blocking Agent on the *In vitro* Growth of IMR-32

Preliminary tests using the cell cycle blocking agents mitomycin C, adriamycin and tamoxifen were conducted in order to investigate whether irreversible blocks of the cell cycle resulting from different mechanisms would alter the bands at 970 cm^{-1}, the symmetric and the asymmetric phosphate stretching regions of nucleic acids. In addition, a reversible cell cycle inhibitor (aphidicolin) was used to mimic the effect of cAMP and

tRA on growth arrest. The growth inhibitory effects of these four cell cycle blocking agents were determined in IMR-32 cells using cell cycle and morphological analysis. These inhibitors not only provided a tool for analysing the different steps in DNA synthesis, but are also valuable therapeutic agents in the treatment of neuroblastoma. Furthermore, the growth inhibitory activities of these agents may enable us to determine whether the symmetric and asymmetric phosphate stretching bands are really indicative of mitotic potential.

Flow cytometric analysis was conducted on the cell population. It provided information on the distribution of the cells among the three phases of the cell cycle, namely the G_0/G_1 phase, the S phase and the G_2/M phase. Data were obtained before and after treatment with aphidicolin and mitomycin C to investigate the effects of these agents. Morphological analysis were done on the effects of adriamycin and tamoxifen on the *in vitro* growth of IMR-32 cells. Although it is well known that aphidicolin, mitomycin C, adriamycin and tamoxifen are capable of inducing cell cycle arrest among various tumor cell lines, their site of action in the cell cycle, their mechanism of action, the associated morphological changes and the relative extent of the inhibition differed among these drugs. The mechanism of action of these inhibitors are indicated below.

Aphidicolin: is a tetracyclic diterpenoid that reversibly inhibits eukaryotic DNA replication by acting directly on the replicative DNA polymerase of eukaryotic cells (Spadari *et al.*, 1982).

Mitomycin C: acts by blocking DNA synthesis. The block results from the cross-linking of guanine in double stranded DNA, and ends in an impediment of cell mitosis that finally leads to cell death regardless of the cell lineage (Takahashi *et al.*, 1998).

Adriamycin: is an anthracycline antibiotic. The primary action of this chemotherapeutic agent is intercalation with DNA, by which many functions of DNA are affected, including DNA and RNA synthesis. Generation of free radicals, resulting from the formation of semiquinone radical intermediates, also plays an important role in the cytotoxicity of this agent (Tamura *et al.*, 1992).

Tamoxifen: 1-(p-dimethylaminoethoxyphenyl)-1,2-diphenyl-1-butene) is a drug known to have TGF–β modulatory and PKC inhibitory effects. Growth inhibition by tamoxifen was associated with inhibition of Ca^{2+}/phospholipid-dependent PKC activity, which preceded the induction of the cell cycle inhibitory protein $p21^{waf1/cip1}$ (Rohlff *et al.*, 1998).

3.4.1 Cell Cycle Analysis

In this study, IMR-32 cells were exposed to aphidicolin at two different concentrations (1 μg/ml and 0.6 μg/ml) and mitomycin C at a concentration of 10 μg/ml. The stage of the cell cycle at which cell growth was arrested was investigated by flow cytometry and the results are shown in Table 3.3. The results indicate clearly that the two doses of aphidicolin block the cell cycle at the S or the S/G_2 phases. The effects were dose-dependent. By comparing control and aphidicolin treated IMR-32 cells, it was found that the block was reversible after removing the drug. In the absence of aphidicolin, the cells completed the cell cycle as the subpopulation at the G_2 phase (47.2%) re-entered into the G_1 subpopulation following mitosis (51.3%). In contrast, mitomycin C blocked the cell cycle in an irreversible manner and the cells were found to accumulate at the G_1/S phase. These experiments allowed us to determine the optimal doses to be used for FTIR studies.

Table 3.3

Effect of aphidicolin and mitomycin C on cell cycle progression in human neuroblastoma cell line-IMR-32[a]

Treatment	Duration of treatment (h)	Percentage distribution		
		G_1	S	G_2+M
Control (untreated)	24	33.3	59.5	7.20
Mitomycin C (10 μg/ml)	3	51.3	48.7	0.00
Aphidicolin (1 μg/ml)	24	5.0	47.8	47.20
Aphidicolin (0.6 μg/ml)	24	7.4	79.0	13.60
After removal of drug	**Time (h)**	**Percentage distribution**		
		G_1	S	G_2+M
Control (untreated)	48	45.0	41.2	13.80
Mitomycin C (10 μg/ml)	48	57.1	38.1	4.80
Aphidicolin (1 μg/ml)	24	51.3	43.1	5.60
Aphidicolin (0.6 μg/ml)	24	41.6	46.5	11.90

a. Percentage of cells in cell cycle phase after treatment with aphidicolin and mitomycin C at various time periods. The data presented is from a representative experiment.

3.4.2 Morphological Analysis

IMR-32 cells were treated with adriamycin at three different concentrations (1 μg/ml, 2.5 μg/ml and 5.0 μg/ml) and with tamoxifen at three different concentrations (1 μM, 5 μM, and 10 μM) in order to select the optimal concentration. Morphological changes due to these agents were studied by phase contrast microscopy. The cells were judged to be apoptotic on the basis of their morphological appearance. However, this type of apoptotic cell death can be further confirmed by biochemical analyses such as DNA fragmentation and TUNEL method.

In the course of this study, it was found that tamoxifen at concentrations of 5 μM (Figure 3.15A) and 10 μM (Figure 3.15B) induced apoptosis in IMR-32 cells within 48 hours whereas cells treated with 1 μM tamoxifen continued to grow after treatment. The effects were dose dependent. The first visible evidence of apoptosis is condensation of chromatin within the nucleus followed by cell shrinkage, blebbing of the plasma membrane, appearance of splitted neurites and later cell ghosts. In the case of adriamycin, it was found that, at concentrations of 2.5 μg/ml (Figure 3.15C, D) and 5.0 μg/ml, treated IMR-32 cells underwent apoptosis within 48 hours, whereas cells treated with 1.0 μg/ml continued to grow even after treatment. The effects were also dose dependent. The optimal dose selected could be used for our future spectroscopic studies.

Figure 3.15 Phase contrast photomicrographs of IMR-32 cells after treatment with adriamycin and tamoxifen for 24 hours. The IMR-32 cells become flattened and undergo apoptosis as evidenced by cell shrinkage, blebbing of the plasma membrane and condensation of the chromatin within the nucleus. The figures (A), (B), (C) and (D) show varying degree of apoptosis depending on the concentration of the drug.

(A) 5 μM tamoxifen treated IMR-32 cells. Original magnification x 150.
(B) 10 μM tamoxifen treated IMR-32 cells. Original magnification x 300.
(C) 2.5 μg/ml adriamycin treated IMR-32 cells. Original magnification x 150.
(D) 2.5 μg/ml adriamycin treated IMR-32 cells. Original magnification x 150.

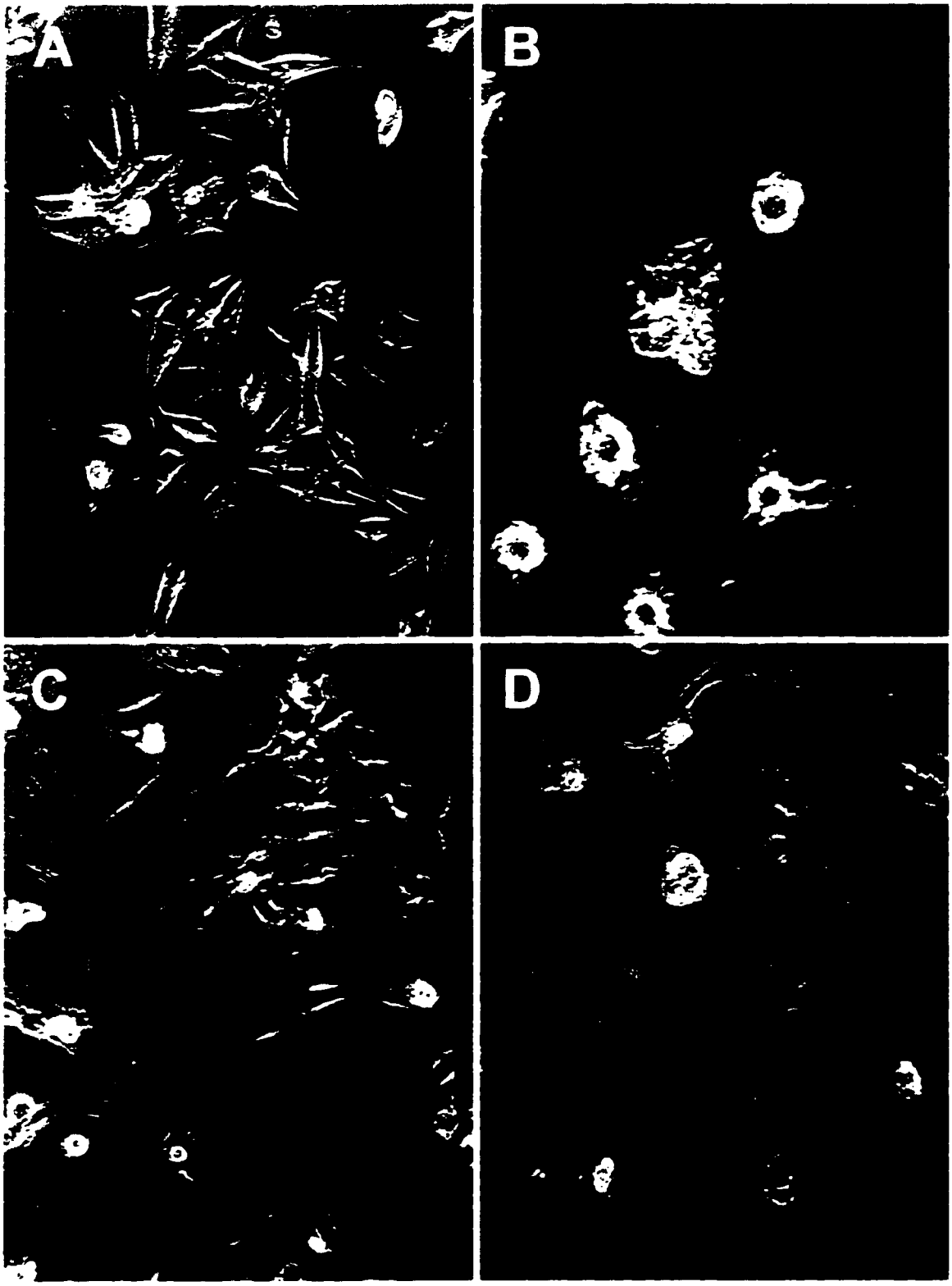
A
B
C
D

CHAPTER 4

DISCUSSION AND FUTURE DIRECTIONS

4.1 Discussion

The aim of this work was to test the hypothesis that the diagnostic bands in the FTIR spectrum accurately reflect the mitotic ability of tumor cells and that treatment with differentiation inducers leads to spectral changes characteristic of normal cells. The approach chosen involved examining the effects of cAMP and tRA inducers on a variety of parameters associated with the differentiation response of the neuronal phenotype. The results obtained reveal that cAMP and tRA at non-toxic concentrations promoted morphological differentiation in the human NB cell line IMR-32 as in other NB cell lines (Sidell, 1982; Gaetano *et al.*, 1991; Thiele, 1991; Linnala *et al.*, 1997). Differentiated IMR-32 cells first emitted long cellular processes (neurites) and later formed pseudoganglia. Growth rate of morphologically differentiated IMR-32 cells was drastically reduced when compared to actively proliferating original cancer cells. The cells then reached a quiescent stage. Thereafter the size of the cell population remained constant. Morphologically differentiated IMR-32 cells exited the cell cycle seven days after treatment and remained quiescent over the following three weeks. The results obtained in our current study correlates well with previous studies which demonstrated that RA induces growth inhibition and morphological differentiation in some NB cell lines characteristic of normal differentiated neuronal cells (Sidell, 1982; Gaetano *et al.*, 1991; Thiele, 1991; Linnala *et al.*, 1997). It has been found that morphological differentiation of IMR-32 cells is associated with changes in the expression level of

markers of differentiation. An increase in the relative expression of NSE as well as TH and a decrease in the intracellular level of CAT were observed (Phipps *et al.*, 1997). The overall findings indicate that IMR-32 cells appeared to be differentiated, according to both morphological and biochemical criteria. Moreover, morphological and biochemical changes are further accompanied by neurofilament protein expression, especially the 200 kDa subunit in differentiated IMR-32 cells. This finding is supported by earlier studies which demonstrated that morphological differentiation of neuroblastoma cells were accompanied by increases in the expression of neurofilament mRNA or protein following RA treatment (Thiele, 1991; Linnala *et al.*, 1997).

However, infrared spectroscopic results indicate that the fully differentiated IMR-32 cells display the same spectral characteristics as untreated (actively proliferative) IMR-32 cells specifically with reference to the nucleic acid region. This may reflect the mitotic ability of differentiated IMR-32 cells, although these exhibit several characteristics of mature neuronal phenotype. These findings further suggest that these two inducers were effective in controlling growth of IMR-32 cells as long as they remained in the culture medium. When challenging the differentiated IMR-32 cells to grow under appropriate conditions, they regained their proliferative capacity. These results further show that IMR-32 cells differentiated at the morphological and molecular level were reverted back to original cancer cells on the basis of morphological as well as FTIR spectral characteristics. This retro-differentiation phenomenon is in agreement with previous studies which demonstrated that the growth inhibitory activity of retinoids was reversible in many tumor systems within 48 hours after removal of the drug (Sidell, 1982).

A similar phenomenon of retro-differentiation was also observed by Lovat *et al.* (1997) for human neuroblastoma cell line SH-SY-5Y using tRA as a differentiation inducer. In their experiments, SH-SY-5Y cells were treated with 1 μM tRA for 5 days and then incubated in the absence of tRA for a further 6 days. It was found that within 2-4 days after withdrawal of tRA the cells re-acquired their proliferative capacity and their structure reverted back to their original morphology. In the same study the authors found that SH-SY-5Y cells, when treated with 1 μM 9-*cis*-retinoic acid under similar experimental conditions, underwent apoptosis after withdrawal of the drug from the medium. Although both retinoic acid isomers induced morphological differentiation of SH-SY-5Y cells, the results obtained from Lovat *et al.* (1997) suggest that the continued presence of retinoic acid is required for the maintenance of a differentiated phenotype in SH-SY-5Y cells.

The spectroscopic results obtained in the present study, especially at the nucleic acid region, suggest that the differentiation inducers (cAMP and tRA) are not capable of inducing terminal exit of the neurons from the cell cycle, although they promote morphological and molecular differentiation as well as arresting growth. Although the morphogen retinoic acid (RA) is currently used in differentiation based therapy for neuroblastoma, previous studies have shown that it does not terminally differentiate all neuroblastoma cell lines *in vitro*, suggesting limitations to its effects. Despite these apparent limitations, relatively little is known regarding the potential actions of RA on the behaviour of neuroblastoma cells resistant to the terminal differentiating effects of this agent (Tiberio *et al.*, 1997). Terminal differentiation of neurons has been found to be coupled with an irreversible withdrawal from the cell cycle (Puri *et al.*, 1997). An

elevation of the intracellular level of adenosine 3':5'- cyclic monophosphate (cAMP) in murine neuroblastoma cells in culture, induced by either prostaglandin E_1 (PGE_1), a stimulator of adenylate cyclase, or by 4-(3-butoxy-4-methoxybenzyl)-2-imidazolidinone (Ro 20-1724), an inhibitor of cyclic nucleotide phosphodiesterase, induces terminal differentiation in many of these cells (La Rosa *et al.*, 1996). However it was not tested whether the differentiation was really terminal, i.e. associated with cell cycle exit in their studies.

The overall findings in our studies indicate that the continued presence of cAMP and tRA is required for the maintenance of a differentiated phenotype as well as growth inhibition in IMR-32 cells. However, the spectral results related to changes in the Amide I band region reflect the drastic cytosolic molecular modification which occur during the differentiation process. These results also indicate that FTIR spectroscopy may be used as a potential diagnostic tool in monitoring molecular changes during treatment of patients with neuroblastoma. There are obvious advantages in using infrared spectroscopy as a powerful diagnostic tool, over the conventional pathology method in screening and diagnosis. It is rapid, accurate, inexpensive, automatable and it requires a minimal amount of sample (Wong *et al.*, 1991_c).

With regards to spectroscopic results, these findings indicate that several important IR spectroscopic changes are associated with the differentiation of IMR-32 cells, as follows:

1. The presence of a band at 970 cm^{-1} in untreated (actively growing) IMR-32 cells indicate its malignant nature. A similar spectral feature was also observed by Wong *et al.* (1991_a) in human cervical cancer and they suggested that it might serve as a key indicator

for malignancy. However, this band was observed here in both untreated and treated IMR-32 cells. Two alternative explanations can be proposed for this finding:

a. The 970 cm^{-1} band could be characteristic of all cells of neural crest origin, irrespective of their malignancy.

b. The fully differentiated IMR-32 cells exhibit spectral characteristics similar to those of original cancer cells even after differentiation.

2. Previous studies have shown that the amount of glycogen is dramatically decreased in exfoliated cells from cancerous cervical tissue compared with those from normal cervical tissue. Cancers of two organs normally rich in glycogen, the vagina and the liver, display a similar spectroscopic pattern, but this pattern is not seen in colon cancer (Wong *et al.*, 1991_a). Similarly, the spectral results obtained in our study indicating no significant changes in the intensity of the glycogen bands between untreated and treated IMR-32 cells raise the possibility that these cells are poor in glycogen content. Hence the glycogen band effect cannot be considered as an important factor in distinguishing the differentiated IMR-32 cells from the actively growing IMR-32 cells.

3. The frequency of the symmetric phosphate stretching band at 1086-1087 cm^{-1} in differentiated IMR-32 cells reflect the malignant nature of these cells even after differentiation (Wong *et al.*, 1991_c; Wong *et al.*, 1993_a; Wong *et al.*, 1993_c).

4. The hydrogen bonding of phosphodiester groups of nucleic acids increased in differentiated IMR-32 cells. Previous studies showed that hydrogen bonding of phosphodiester groups of nucleic acids increased in cancers of other organs such as cervix, colon, liver, vagina, breast, skin, stomach and esophagus and are common to all human malignancies examined to date (Wong *et al.*, 1991_c; Wong *et al.*, 1993_a; Wong *et*

al., 1993_c). Therefore the increase in the hydrogen bonding of phosphodiester groups of nucleic acids in differentiated IMR-32 cells is in good agreement with the fact that the observed differentiation is not terminal and that the cells can re-enter the mitotic cycle upon growth challenge.

5. Normally one would expect some spectral differences in the secondary structure of proteins between the normal and malignant cells or tissue. Previous studies conducted with normal and malignant human colon tissue have shown that the ratio between the β-sheet segments and the α-helix segments becomes smaller in the malignant tissue, as indicated by the decrease in the intensity ratio between the 1637 cm^{-1} and the 1654 cm^{-1} band (Wong *et al.*, 1993_a). However, the spectroscopic results obtained in our study revealed no such changes between β-sheet and α-helix segments in the secondary structure of proteins of untreated (actively growing) and treated (differentiated) IMR-32 cells.

The spectral results indicating changes at the amide I band region of the differentiated IMR-32 cells when compared to the original cancer cells is different from the observations of Wong *et al.* (1993_a) where human colonic tissues were used. When the authors studied normal and malignant colonic tissues in the amide I band region, they found that the relative intensity of the 1612 cm^{-1} band in the malignant tissue decreases when compared to the normal tissue. Their findings showed a reduction of intermolecular hydrogen-bond aggregation between neighboring protein molecules during the process of malignant transformation. However, a different spectral effect was observed in our studies. This probably relates to the molecular changes associated with the mature phenotype of treated IMR-32 cells.

The following two factors may contribute to the lack of effectiveness of these inducers in causing irreversible exit from the cell cycle are:

1. The cell line used in these studies was established from highly malignant tumor with an amplified N-myc (25 copies). This is supported by previous studies which showed that transient inhibition of cell growth and N-myc expression occurs in the N-myc gene amplified SMS-KCNR line following treatment with retinoic acid. In contrast, the neuroblastoma cell line (SMS-LHN) which overexpresses N-myc without gene amplification responds to retinoic acid with a prolonged growth arrest (>60 days) and this growth arrest is correlated with decreased N-myc protein expression (Reynolds *et al.*, 1991).

2. Lack of expression of a functional high affinity nerve growth factor receptor (trk-A) which leads to poor prognosis. Previous studies have shown that trk-A expressing HTLA 230 cells terminally differentiate into mature neurons in the presence of NGF in culture and that the activation of a functional NGF signal cascade results in reversion of the advanced NB into benign ganglioneuroblastoma (Matsushima and Bogenmann, 1994). Similar results were obtained *in vitro* using the SH-SY-5Y neuroblastoma strain (Jensen *et al.*, 1992).

4.2 Future Developments

In these studies, it was shown that aphidicolin at concentrations of 0.6 μg/ml and 1.0 μg/ml was capable of arresting cell cycle in a reversible manner. Our results are in agreement with earlier reports which showed that both the inhibition of DNA

polymerase α *in vitro* and the inhibition of cell growth observed *in vivo* are reversible (Spadari *et al.*, 1982).

Mitomycin C at a concentration of 10 μg/ml stopped the cell cycle in an irreversible manner. It was reported earlier that mitomycin C remains in DNA for a long time and kills cells which have the potential to divide (Takahashi *et al.*, 1998). However, FTIR experiments need to be performed in the near future to determine whether the cell proliferation potential after treatment with aphidicolin and mitomycin C can be measured using this technique.

The two other irreversible cell cycle blocking agents, adriamycin and tamoxifen showed promise in the preliminary tests based on morphological analysis. Tamoxifen at concentrations of 5 μM and 10 μM were found to induce apoptosis in IMR-32 cells within 48 hours. These results agree with previous studies by Ercoli *et al.* (1998) which showed that tamoxifen significantly inhibited the growth of ER^- ovarian cancer cell line A2780, and induced apoptosis in these cells. Similarly, IMR-32 cells treated with adriamycin at concentrations of 2.5 μg/ml and 5.0 μg/ml died of apoptosis within 48 hours. The results of these studies indicate that these two chemical agents force human neuroblastoma cell line IMR-32 to enter the apoptotic cell death (programmed cell death). Apoptosis induction as well as cell cycle block are the consequence of DNA damages induced by these cell cycle inhibitors. Detailed FTIR analysis were not conducted and will be required in future studies to confirm these morphological findings.

These studies (morphological and cell cycle analysis) indicate a need for future experiments to determine whether the FTIR spectral characteristics are a good indicator of the actual growth potential of tumor cells. If so, no changes should occur in the

symmetric and asymmetric phosphate stretching region upon cell exposure to the reversible cell cycle inhibitors (which mimics cAMP and tRA) effect. In contrast, spectra similar to those of normal cells should be observed when tumor cells are exposed to irreversible cell cycle blocking agents or at least changes indicating DNA damages induced by the inhibitors.

For future work, we plan to repeat these experiments with another human neuroblastoma cell line SH-SY-5Y (which terminally differentiate) under the conditions described in this work.

CHAPTER 5

CONCLUSIONS

We set out with a goal to verify whether differentiation of human neuroblastoma IMR-32 cells following induction with tRA and cAMP would alter the FTIR spectral characteristics of cancer cells. In the course of the study, it was demonstrated that tRA and cAMP, at optimal dose concentrations, induced alterations in cell morphology (emission of neurites and formation of pseudoganglia) associated with cell growth inhibition following treatment. It was found that morphologically differentiated IMR-32 cells exited the cell cycle seven days after treatment and remained quiescent over the following three weeks. The Western-blot analysis method further confirmed the morphological results and demonstrated that the acquisition of a mature neuronal phenotype in treated IMR-32 cells was accompanied by an increase in the expression of neurofilament protein especially the 200 kDa subunit as found in other studies. Thus, the treated IMR-32 cells met all the morphological and biochemical criteria associated with terminal differentiation. These features were also reflected on the FTIR spectra. Differentiated IMR-32 cells exhibited changes in the amide I band region of the spectrum between untreated and treated IMR-32 cells reflecting the drastic cytosolic molecular modifications which occur during the differentiation process.

The infrared spectroscopic results, however, demonstrated that the fully differentiated IMR-32 cells exhibit the same spectral characteristics as untreated (actively growing) IMR-32 cells, especially in the symmetric and asymmetric phosphate stretching region of the phosphodiester groups of nucleic acids. This spectral data indicates that,

despite differentiation, the neoplastic nature is maintained in IMR-32 cells although they exhibit several characteristic of the mature neuronal phenotype.

The above findings motivated us to investigate whether the spectral characteristics in the region of symmetric and asymmetric phosphate stretching region is associated with mitotic ability. Upon challenge to grow under appropriate conditions, the differentiated IMR-32 cells resumed proliferation at the same rate as original cancer cells. Simultaneously the cells retracted their neurites and the final morphological structure looked similar to that of the original cancer cells. The infrared spectra of the retro-differentiated IMR-32 cells showed the same spectral characteristics at the symmetric, asymmetric and amide I band region when compared with that of actively growing cells.

It can be concluded from the above findings that, although the two inducers (cAMP and tRA) promote morphological and molecular differentiation as well as growth inhibition in IMR-32 cells, they were not capable of inducing terminal exit of neurons from the cell cycle and that the FTIR spectra reliably identified the neoplastic nature of these cells. Moreover, the spectral characteristics corresponding to the region of symmetric and asymmetric phosphate stretching band may be related to the mitotic potential of cells.

REFERENCES

Alitalo, K., Koskinen, P., Makela, T. P., Saksela, K., Sistonen, K., and Winqvist, R. (1987) Myc oncogenes: Activation and amplification. Biochim. Biophys. Acta, **907**, 1-32.

Azar, C. G., Scavarda, N. J., Reynolds, C. P., and Brodeur, G. M. (1990) Multiple defects of the nerve growth factor receptor in human neuroblastomas. Cell Growth Differ., **1**, 421-428.

Azar, C. G., Scavarda, N. J., Nakagawara, A., and Brodeur, G. M. (1994) Expression and function of the nerve growth factor receptor (trk-A) in human neuroblastoma cell lines. In: Advances in Neuroblastoma Research 4 Ed.: Evans, A. E., D'Angio, G. J., Biedler, J. L., Brodeur, G. M., Nakagawara, A. (Wiley-Liss, New York) pp 169-175.

Bates, S., Mickley, L., Chen, Y., Richercht, N., Rudick, J., Biedler, J., and Fojo, A. T. (1989) Expression of a drug resistance gene in human neuroblastoma cell lines: Modulation by retinoic acid-induced differentiation. Mol. Cell. Biol., **9**, 4337-4344.

Biedler, J. L., Casals, D., Chang, T. D., Meyers, M. B., Spengler, B. A., and Ross, R. A. (1991) Multidrug-resistant human neuroblastoma cells are more differentiated than controls and retinoic acid further induces lineage-specific differentiation. In: Advances in Neuroblastoma Research 3 Ed.: Evans, A. E., D'Angio, G. J., Knudson, A. G., Seeger, R. C. (Wiley-Liss, New York) pp 181-191.

Boylan, J. F., and Gudas, L. J. (1991) Overexpression of the cellular retinoic acid binding protein-I (CRABP-I) results in a reduction in differentiation-specific gene expression in F9 teratocarcinoma cells. J. Cell Biol., **112**, 965-979.

Bradford, M. M. (1976) A rapid and sensitive method for the quantitation of microgram quantities of protein utilizing the principle of protein-dye binding. Analytical Biochemistry, **72**, 248-254.

Braiman, M. S., and Rothschild, K. J. (1988) Fourier transform infrared techniques for probing membrane protein structure. Ann. Rev. Biophys. Biophys. Chem., **17**, 541-570.

Brodeur, G. M. (1991) In: Biochemical and Molecular Aspects of Selected Cancers 1 Ed.: Thomas, G. P., Theresa, P. P. (Academic Press, Inc, New York) pp 251-276.

Brodeur, G. M., Pritchard, J., Berthold, F., Carlsen, N. L. T., Castel, V., Castleberry, R. P., De Bernardi, B., Evans, A. E., Favrot, M., Hedborg, F., Kaneko, M., Kemshead, J., Lampert, F., Lee, R. E. J., Look, A. T., Pearson, A. D. J., Philip, T., Roald, B., Sawada, T., Seeger, R. C., Tsuchida, Y., and Voute, P. A. (1993) Revisions of the international criteria for neuroblastoma diagnosis, staging and response to treatment. Journal of Clinical Oncology, **11**, 1466-1477.

Cameron, D. G., and Moffatt, D. J. (1984) Deconvolution, derivation, and smoothing of spectra using Fourier transforms. Journal of Testing and Evaluation, **12**, 78-85.

Chao, M. V. (1992) Neurotrophin receptors: A window into neuronal differentiation. Neuron, **9**, 583-593.

Chen, J., Chattopadhyay, B., Venkatakrishnan, G., and Ross, A. H. (1990) Nerve growth factor-induced differentiation of human neuroblastoma and neuroepithelioma cell lines. Cell Growth Differ., **1**, 79-85.

Ciccarone, V., Spengler, B. A., Meyers, M. B., Biedler, J. L., and Ross, R. A. (1989) Phenotypic diversification in human neuroblastoma cells: Expression of neural crest lineages. Cancer Res., **49**, 219-225.

Cooper, M. J., Hutchins, G. M., Cohen, P. S., Helman, L. J., Mennie, R. J., and Israel, M. A. (1990) Human neuroblastoma tumor cell lines correspond to the arrested differentiation of chromaffin adrenal medullary neuroblasts. Cell Growth Differ., **1**, 149-159.

De Bold, C. R., Menefee, J. K., Nicholson, W. E., and Orth, D. N. (1988) POMC gene is expressed in many normal human tissues and in tumors, not associated with the ectopic adrenocorticotropin syndrome. Mol. Endocrinol., **2**, 862-870.

Di Martino, D., Ponzoni, M., Cornaglia-Ferraris, P., and Paolo Tonini, G. (1990) Different regulation of mid-size neurofilament and N-myc mRNA expression during neuroblastoma cell differentiation induced by retinoic acid . Cell. Mol. Neurobiol., **10**, 459-470.

Ercoli, A., Scambia, G., Fattorossi, A., Raspaglio, G., Battaglia, A., Cicchillitti, L., Malorni, W., Rainaldi, G., Panici, P. B., and Mancuso, S. (1998) Comparative study on the induction of cytostasis and apoptosis by ICI 182, 780 and tamoxifen in an estrogen receptor-negative ovarian cancer cell line. Int. J. Cancer, **76**, 47-54.

Evans, R. (1988) The steroid and thyroid hormone receptor superfamily. Science, **240**, 889-895.

Fesus, L., Davies, P. J. A., and Piacentini, M. (1991) Apoptosis: Molecular mechanisms in programmed cell death. Eur. J. Cell Biol., **56**, 170-177.

Gaetano, C., Matsumoto, K., and Thiele C. J. (1991) Retinoic acid resistant neuroblastoma cells and the expression of IGF-2. In: Advances in Neuroblastoma Research 3 Ed.: Evans, A. E., D'Angio, G. J., Knudson, A. G., Seeger, R. C. (Wiley-Liss, New York) pp 165-172.

Gaetano, C., Matsumoto, K., and Thiele, C. J. (1992) *In vitro* activation of distinct molecular and cellular phenotypes after induction of differentiation in a human neuroblastoma cell line. Cancer Res., **52**, 4402-4407.

Giguere, V., Lyn, S., Yip, P., Siu, C. H., and Amin, S. (1990) Molecular cloning of cDNA

encoding a second cellular retinoic acid-binding protein. Proc. Natl. Acad. Sci., U.S.A., **87**, 6233-6237.

Griffiths, P. R., and Pariente, G. L. (1986) Introduction to spectral deconvolution. Trends in Analytical Chemistry, **5**, 209-215.

Gudas, L. J. (1992) Retinoids, retinoid-responsive genes, cell differentiation and cancer. Cell Growth Differ., **3**, 655-662.

Haber, M., Madafiglio, J., Bordow, S. B., Gilbert, J., Cheung, B., Marshall, G. M., and Norris, M. D. (1994) Expression of retinoic acid-responsive genes in primary neuroblastomas. In: Advances in Neuroblastoma Research 4 Ed.: Evans, A. E., D'Angio, G. J., Biedler, J. L., Brodeur, G. M., Nakagawara, A. (Wiley-Liss, New York) pp 245-251.

Hartmann, O., Pinkerton, C., Zucker, J. M., Philip, T., and Breatnach, F. (1988) Very high dose cisplatin and etoposide in children with untreated advanced neuroblastoma. Journal of Clinical Oncology, **6**, 44-50.

Helman, L. J., Thiele, C. J., Linehan, W. M., Nelkin, B. D., Baylin, S. B., and Israel, M. A. (1987) Molecular markers of neuroendocrine development and evidence of environmental regulation. Proc. Natl. Acad. Sci., U.S.A., **84**, 2336-2339.

Jackson, M., Haris, P. I., and Chapman, D. (1989) Fourier transform infrared spectroscopic studies of lipids, polypeptides and proteins. Journal of Molecular Structure, **214**, 329-355.

Jensen, L. M., Zhang, Y., and Shooter, E. M. (1992) Steady-state polypeptide modulations associated with nerve growth factor (NGF)-induced terminal differentiation and NGF deprivation-induced apoptosis in human neuroblastoma cells. The Journal of Biological Chemistry, **267**, 19325-19333.

Judware, R., and Culp, L. A. (1995) Over-expression of transfected N-myc oncogene in human SKNSH neuroblastoma cells down-regulates expression of β1 integrin subunit. Oncogene, **113**, 2599-2607.

Keim, D. R., Hailat, N., Kuick, R., Reynolds, C. P., Brodeur, G. M., Seeger, R. C., and Hanash, S. M. (1993) PCNA levels in neuroblastoma are increased in tumors with an amplified N-myc gene and in metastatic stage tumors. Clin. Exp. Metastasis, **11**, 83-90.

Keshelava, N., Seeger, R. C., and Reynolds, C. P. (1997) Drug resistance in human neuroblastoma cell lines correlates with clinical therapy. European Journal of Cancer, **33**, 2002-2006.

Kogner, P., Barbany, G., Persson, H., Soderhall, S., Ahstrom, L., and Bjork, O. (1994) Expression of nerve growth receptor mRNAs and clinical response to retinoic acid in neuroblastoma. In: Advances in Neuroblastoma Research 4 Ed.: Evans, A. E., D'Angio,

G. J., Biedler, J. L., Brodeur, G. M., Nakagawara, A. (Wiley-Liss, New York) pp 147-153.

Kogner, P., Borgstrom, P., Bjellerup, P., Schilling, F. H., Refai, E., Jonsson, C., Dominici, C., Wassberg, E., Bihl, H., Jacobsson, H., Theodorsson, E., and Hassan, M. (1997) Somatostatin in neuroblastoma and ganglioneuroma. European Journal of Cancer, **33**, 2084-2089.

Koizumi, H., Wakisaka, M., Nakada, K., Takakuwa, T., Fujioka, T., Yamate, N., and Uchikoshi, T. (1995) Demonstration of apoptosis in neuroblastoma and its relationship to tumor regression. Virchows Arch., **427**, 167-173.

Krishan, A. (1975) Rapid flow cytometric analysis of mammalian cell cycle by propidium iodide staining. J. Cell Biol., **66**, 188-193.

Kauppinen, J. K., Moffatt, D. J., Mantsch, H. H., and Cameron, D. G. (1981) Fourier transforms in the computation of self-deconvoluted and first-order derivative spectra of overlapped band contours. Anal. Chem., **53**, 1454-1457.

La Rosa, F. G., Kumar, S., and Prasad, K. N. (1996) Increased expression of ubiquitin during adenosine 3', 5'-cyclic monophosphate-induced differentiation of neuroblastoma cells in culture. J. Neurochem., **66**, 1845-1850.

Laemmli, U. K. (1970) Cleavage of structural proteins during the assembly of the head of bacteriophage T4. Nature, **227**, 680-685.

Lambert, J. B., Shurvell, H. F., Lightner, D. A., and Graham Cooks, R. (1987) In: Introduction to Organic Spectroscopy (Macmillan Publishing Company, New York) pp 135-158.

Lando, M., Abemayor, E., Verity, M. A., and Sidell, N. (1990) Modulation of intracellular cyclic adenosine monophosphate levels and the differentiation response of human neuroblastoma cells. Cancer Res., **50**, 722-727.

Li, C., Einhorn, P. A., and Reynolds, C. P. (1994) Expression of retinoic acid receptors α, β, and γ in human neuroblastoma cell lines. In: Advances in Neuroblastoma Research 4 Ed.: Evans, A. E., D'Angio, G. J., Biedler, J. L., Brodeur, G. M., Nakagawara, A. (Wiley-Liss, New York) pp 221-227.

Linnala, A., Lehto, V. P., and Virtanen, I. (1997) Neuronal differentiation in SH-SY-5Y human neuroblastoma cells induces synthesis and secretion of tenascin and upregulation of α_v integrin receptors. Journal of Neuroscience Research, **49**, 53-63.

Lotan, R., Lotan, D., and Sacks, P. G. (1990) Inhibition of tumor cell growth by retinoids. Methods in Enzymology, **190**, 100-111.

Lovat, P. E., Irving, H., Petruzzelli, M. A., Bernassola, F., Malcolm, A. J., Pearson, A. D.

J., Melino, G., and Redfern, C. P. F. (1997) Retinoids in neuroblastoma therapy: Distinct biological properties of 9-*cis*- and all-*trans*-retinoic acid. European Journal of Cancer, **33**, 2075-2080.

Lucarelli, E., Kaplan, D., Matsumoto, K., Sickafuse, S., and Thiele, C. J. (1994) Retinoic acid induced differentiation is mediated by Trk-B receptors. In: Advances in Neuroblastoma Research 4 Ed.: Evans, A. E., D'Angio, G. J., Biedler, J. L., Brodeur, G. M., Nakagawara, A. (Wiley-Liss, New York) pp 185-198.

Lucarelli, E., Kaplan, D., and Thiele, C. J. (1997) Activation of trk-A but not trk-B signal transduction pathway inhibits growth of neuroblastoma cells. European Journal of Cancer, **33**, 2068-2070.

Manohar, C., Salwen, H., Furtado, M., and Cohn, S. (1994) Retinoic acid induced expression of homeobox genes in human neuroblastoma cells. Prog. Clin. Biol. Res., **385**, 229-235.

Matsushima, H., and Bogenmann, E. (1994) NGF induces terminal differentiation in trk-A expressing neuroblastoma cells *in vitro* and *in vivo*. In: Advances in Neuroblastoma Research 4 Ed.: Evans, A. E., D'Angio, G. J., Biedler, J. L., Brodeur, G. M., Nakagawara, A. (Wiley-Liss, New York) pp 177-183.

McCaffery, P., and Drager, U. C. (1994) Hot spots of retinoic acid synthesis in the developing spinal cord. Proc. Natl. Acad. Sci., U.S.A., **91**, 7194-7197.

Melino, G., Farrace, M. G., Ceru, M. P., and Piacentini, M. (1988) Correlation between transglutaminase activity and polyamine levels in retinoic acid and a difluoro methylornithine induced differentiation of human neuroblastoma cells. Experimental Cell Research, **179**, 429-445.

Melino, G., Thiele, C. J., Knight, R. A., and Piacentini, M. (1997) Retinoids and the control of growth/death decisions in human neuroblastoma cell lines. Journal of Neuro-Oncology, **31**, 65-83.

Nakagawara, A., Arima, M., Azar, C. G., Scavarda, N. J., and Brodeur, G. M. (1992) Inverse relationship between trk expression and N-myc amplification in human neuroblastoma. Cancer Res., **52**, 1364-1368.

Nakagawara, A., Arima-Nakagawara, M., Scavarda, N. J., Azar, C. G., Cantor, A. B. and Brodeur, G. M. (1993) Association between high levels of expression of the trk gene and favourable outcome in human neuroblastoma. New Engl. J. Med., **328**, 847-854.

Nakagawara, A., and Brodeur, G. M. (1997) Role of neurotrophins and their receptors in human neuroblastomas: A primary culture study. European Journal of Cancer, **33**, 2050-2053.

Nakanishi, K., and Solomon, P. H. (1977) In: Infrared Absorption Spectroscopy (Holden-Day, Inc., Oakland) pp 1-13.

Pahlman, S., Odelstad, L., Larsson, E., Grotte, G., and Nilsson, K. (1981) Phenotypic changes of human neuroblastoma cells in culture induced by 12-O-tetradecanoyl-phorbol-13-acetate. Int. J. Cancer, **28**, 583-589.

Pahlman, S., Ruusala, A. I., Abrahamsson, L., Mattsson, M. E. K., and Esscher, T. (1984) Retinoic acid induced differentiation of cultured human neuroblastoma cells: A comparison with phorbolester induced differentiation. Cell Differentiation, **14**, 135-44.

Pedersen, W. A., Becker, L. E., and Yeger, H. (1993) Expression and distribution of peripherin protein in human neuroblastoma cell lines. Int. J. Cancer, **53**, 463-470.

Pence, J. C., and Shorter, N. A. (1991) Further studies on the interaction between vasoactive intestinal peptide and neuroblastoma cell lines. In: Advances in Neuroblastoma Research 3 Ed.: Evans, A. E., D'Angio, G. J., Knudson, A. G., Seeger, R. C. (Wiley-Liss, New York) pp 375-381.

Perez-Polo, J. R., Werrbach-Perez, K., and Tiffany-Castiglioni, E. (1979) A human clonal cell line model of differentiating neurons. Dev. Biol., **71**, 341-355.

Phipps, J., Jouishomme, H., Lacelle, S., and Belbaraka, L. (1997) Gap junctions, Steacie Institute for Molecular Sciences, National Research Council of Canada, Ottawa-unpublished data.

Piacentini, M., Fesus, L., Farrace, M. G., Ghibelli, L., Piredda, L., and Melino, G. (1991) The expression of "tissue" transglutaminase in two human cancer cell lines is related with the programmed cell death (apoptosis). Eur. J. Cell Biol., **54**, 246-254.

Prasad, K. N., Mandal, B., and Kumar, S. (1973) Human neuroblastoma cell culture: Effect of 5-bromodeoxyuridine on morphological differentiation and levels of neural enzymes. Proc. Soc. Exp. Biol. Med., **144**, 38-42.

Prasad, K. N., and Kumar, S. (1975) Role of cyclic AMP in differentiation of human neuroblastoma cells in culture. Cancer, **36**, 1338-1343.

Puri, P. L., Medaglia, S., Cimino, L., Maselli, C., Germani, A., Marzio, E. D., Levrero, M., and Balsano, C. (1997) Uncoupling of p21 induction and myoD activation results in the failure of irreversible cell cycle arrest in doxorubicin-treated myocytes. Journal of Cellular Biochemistry, **66**, 27-36.

Rabinovsky, E. D., Le, W. D., and McManaman, J. L. (1992) Differential effects of neurotrophic factors on neurotransmitter development in the IMR-32 human neuroblastoma cell line. The Journal of Neuroscience, **12**, 171-179.

Reddy, U. R., Pleasure, S., Baker, D., Lee, V. M-Y., Ross, A. H., and Pleasure, D. (1991) Primitive neuroectodermal tumors (PNETS) of the CNS and PNS that express functional nerve growth factor receptors (NGFR) but fail to differentiate in response to NGF. In: Advances in Neuroblastoma Research 3 Ed.: Evans, A. E., D'Angio, G. J., Knudson, A. G., Seeger, R. C. (Wiley-Liss, New York) pp 243-248.

Rettig, W. J., Spengler, B. A., Garin Chesa, P., Old, L. J., and Biedler, J. L. (1987) Coordinate changes in neuronal phenotype and surface antigen expression in human neuroblastoma cell variants. Cancer Res., **47**, 1383-1389.

Reynolds, C. P., Kane, D. J., Einhorn, P. A., Matthay, K. K., Crouse, V. L., Wilbur, J. R., Shurin, S. B., and Seeger, R. C. (1991) Response of neuroblastoma to retinoic acid *in vitro* and *in vivo*. In: Advances in Neuroblastoma Research 3 Ed.: Evans, A. E., D'Angio, G. J., Knudson, A. G., Seeger, R. C. (Wiley-Liss, New York) pp 203-211.

Reynolds, C. P., Schindler, P. F., Jones, D-M., Gentile, J. L., Proffitt, R. T., and Einhorn, P. A. (1994) Comparison of 13-*cis*-retinoic acid to *trans*-retinoic acid using human neuroblastoma cell lines. In: Advances in Neuroblastoma Research 4 Ed.: Evans, A. E., D'Angio, G. J., Biedler, J. L., Brodeur, G. M., Nakagawara, A. (Wiley-Liss, New York) pp 237-244.

Rigas, B., Morgello, S., Goldman, I. S., and Wong, P. T. T (1990) Human colorectal cancers display abnormal Fourier-transform infrared spectra. Proc. Natl. Acad. Sci., U.S.A., **87**, 8140 -8144.

Rigas, B., and Wong, P. T. T (1992) Human colon adenocarcinoma cell lines display infrared spectroscopic features of malignant colon tissues. Cancer Res., **52**, 84-88.

Rohlff, C., Blagosklonny, M. V., Kyle, E., Kesari, A., Kim, I. Y., Zelner, D. J., Hakim, F., Trepel, J., and Bergan, R. C. (1998) Prostate cancer cell growth inhibition by tamoxifen is associated with inhibition of protein kinase C and induction of $p21^{waf1/cip1}$. The Prostate, **37**, 51-59.

Ross, R. A., Spengler, B. A., and Biedler, J. L. (1983) Coordinate morphological and biochemical interconversion of human neuroblastoma cells. J. Natl. Cancer Inst., **71**, 741-747.

Ross, R. A., Ciccarone, V., Meyers, M. B., Spengler, B. A., and Biedler, J. L. (1988) Differential expression of intermediate filaments and fibronectin in human neuroblastoma cells. In: Advances in Neuroblastoma Reseach 2 Ed.: Evans, A. E., D'Angio, G. J., Knudson, A. G., Seeger, R. C. (Wiley-Liss, New York) pp 277-289.

Ross, R. A., Bossart, E., Spengler, B. A., and Biedler, J. L. (1991) Multipotent capacity of morphologically intermediate (I-type) human neuroblastoma cells after treatment with differentiation-inducing drugs. In: Advances in Neuroblastoma Research 3 Ed.: Evans, A. E., D'Angio, G. J., Knudson, A. G., Seeger, R. C. (Wiley-Liss, New York) pp 193-201.

Schmidt, M. L., Kuzmanoff, K. L., Ling-Indeck, L., and Pezzuto, J. M. (1997) Betulinic acid induces apoptosis in human neuroblastoma cell lines. European Journal of Cancer, **33**, 2007-2010.

Schwab, M., Alitalo, K., Klempnauer, K. H., Varmus, H., Bishop, J., Gilbert, F., Brodeur, G., Goldstein, M., and Trent, J. (1983) Amplified DNA with limited homology to myc cellular oncogene is shared by human neuroblastoma cell lines and a neuroblastoma tumour. Nature, **305**, 245-248.

Schwab, M., Varmus, H. E., and Bishop, J. M. (1985) Human N-myc gene contributes to neoplastic transformation of mammalian cells in culture. Nature, **316**, 160-162.

Sharpe, C. R. (1991) Retinoic acid can mimic endogenous signals involved in transformation of the Xenopus nervous system. Neuron, **7**, 239-247.

Sidell, N. (1982) Retinoic acid-induced growth inhibition and morphologic differentiation of human neuroblastoma cells *in vitro*. J. Natl. Cancer Inst., **68**, 589-596.

Sidell, N., Lucas, C. A., and Kreutzberg, G. W. (1984) Regulation of acetylcholinesterase activity by retinoic acid in a human neuroblastoma cell line. Experimental Cell Research, **155**, 305-309.

Sidell, N., and Horn, R. (1985) Properties of human neroblastoma cells following induction by retinoic acid. In: Advances in Neuroblastoma Research Ed.: Evans, A. E., D'Angio, G. J., Seeger, R. C. (Alan R Liss Inc, New York) pp 39-53.

Smith, B. C. (1996) In: Fundamentals of Fourier Transform Infrared Spectroscopy (CRC Press, Florida) pp 1-86.

Sonnenfeld, K. H., and Ishii, D. N. (1982) Nerve growth factor effects receptors in cultured human neuroblastoma cell lines. Journal of Neuroscience Research, **8**, 375-391.

Spadari, S., Sala, F., and Pedrali-Noy, G. (1982) Aphidicolin: a specific inhibitor of nuclear DNA replication in eukaryotes. Trends in Biochemical Sciences, 29-32.

Spengler, B. A., Domenech, C., Porubcin, M., and Biedler, J. L. (1994) Human neuroblastoma lines respond differently to diverse differentiation-inducing agents. In: Advances in Neuroblastoma Research 4 Ed.: Evans, A. E., D'Angio, G. J., Biedler, J. L., Brodeur, G. M., Nakagawara, A. (Wiley-Liss, New York) pp 261-267.

Sugimoto, T., Sawada, T., Matsumura, T., Horii, Y., Hino, T., Kemshead, J. T., Suzuki, Y., Okada, M., and Tagaya, O. (1988) Neuronal differentiation of human neuroblastoma cells by a novel synthetic polyprenoic acid. In: Advances in Neuroblastoma Reseach 2 Ed.: Evans, A. E., D'Angio, G. J., Knudson, A. G., Seeger, R. C. (Wiley-Liss, New York) pp 337-351.

Susi, H., and Byler, D. M. (1986) Resolution-enhanced Fourier transform infrared spectroscopy of enzymes. Methods in Enzymology, **130**, 290-310.

Suzuki, T., Bogenmann, E., Shimada, H., Stram, D., and Seeger, R. C. (1993) Lack of high-affinity nerve growth factor receptors in aggressive neuroblastoma. J. Natl. Cancer Inst., **85**, 377-384.

Tabin, C. J. (1991) Retinoids, homeoboxes, and growth factors: Toward molecular models for limb development. Cell, **66**, 199-217.

Takahashi, N., Murayama, T., Oda, M., and Miyakoshi, M. (1998) Cell growth inhibition and DNA incorporation of mitomycin C in cell culture. Ophthalmic Res., **30**, 120-125.

Tamura, J., Tanaka, J., Fujita, K-I., Yoshida, M., Kasamatsu, T., Arii, S., and Tobe, T. (1992) Effect of anticancer agents on cell cycle of regenerating hepatocytes in rats. Journal of Surgical Research, **53**, 218-226.

Thiele, C. J., Reynolds, C. P., and Israel, M. A. (1985) Decreased expression of N-myc precedes retinoic acid-induced morphological differentiation of human neuroblastoma. Nature, **313**, 404-406.

Thiele, C. J. (1991) Patterns of regulation of nuclear proto-oncogenes MYCN and MYB in retinoic acid treated neuroblastoma cells. In: Advances in Neuroblastoma Research 3 Ed.: Evans, A. E., D'Angio, G. J., Knudson, A. G., Seeger, R. C. (Wiley-Liss, New York) pp 151-156.

Tiberio, A., Farina, A. R., Tacconelli, A., Cappabianca, L., Gulino, A., and Mackay, A. R. (1997) Retinoic acid enhanced invasion through reconstituted basement membrane by human SK-N-SH neuroblastoma cells involves membrane associated tissue type plasminogen activator. Int. J. Cancer, **73**, 740-748.

Tooke, P. B. (1988) Fourier self-deconvolution in infrared spectroscopy. Trends in Analytical Chemistry, **7**, 130-136.

Torii, H., and Tasumi, M. (1996) Theoretical Analyses of the Amide I Infrared Bands of Globular Proteins. In: Infrared Spectroscopy of Biomolecules Ed.: Mantsch, H. H. and Chapman, D. (Wiley-Liss, New York) pp 1-18.

Towbin, H., Staehelin, T., and Gordon, J. (1979) Electrophoretic transfer of proteins from polyacrylamide gels to nitrocellulose sheets: Procedure and some applications. Proc. Natl. Acad. Sci., U.S.A., **76**, 4350-4354.

Usui, T., Nakai, Y., Tsukada, T., Jingami, H., Takahashi, H., and Imura, H. (1989) Expression of adrenocorticotrophin-releasing hormone precursor gene in placenta and in other non-hypothalamic tissues in man. Mol. Endocrinol., **2**, 871-875.

Vignali, G., Niclas, J., Sprocati, M. T., Vale, R. D., Sirtori, C., and Navone, F. (1996) Differential expression of ubiquitous and neuronal kinesin heavy chains during differentiation of human neuroblastoma and PC12 cells. European Journal of Neuroscience, **8**, 536-544.

Wagner, M., Thaller, C., Jassel, T., and Eichele, G. (1990) Polarizing activity and retinoid synthesis in the floor plate of the neuronal tube. Nature, **356**, 819-822.

Waring, L., and Sidell, N. (1991) Differential susceptibilities of spinal cord neurons to retinoic acid-induced survival and differentiation. Dev. Biol., **144**, 429-435.

Wong, P. T. T., Wong, R. K., Caputo, T. A., Godwin, T. A., and Rigas, B. (1991_a) Infrared spectroscopy of exfoliated human cervical cells: Evidence of extensive structural changes during carcinogenesis. Proc. Natl. Acad. Sci., U.S.A., **88**, 10988-10992.

Wong, P. T. T., Papavassiliou, E. D., and Rigas, B. (1991_b) Phosphodiester stretching bands in the infrared spectra of human tissues and cultured cells. Applied Spectroscopy, **45**, 1563-1567.

Wong, P. T. T., Cadrin, M., and French, S. W. (1991_c) Distinctive infrared spectral features in liver tumor tissue of mice: Evidence of structural modifications at the molecular level. Experimental and Molecular Pathology, **55**, 269-284.

Wong, P. T. T., Lacelle, S., and Yazdi, H. M. (1993_a) Normal and malignant human colonic tissues investigated by pressure-tuning FT-IR spectroscopy. Applied Spectroscopy, **47**, 1830-1835.

Wong, P. T. T., Wong, R. K., and Fung, M. F. K. (1993_b) Pressure-tuning FT-IR study of human cervical tissues. Applied Spectroscopy, **47**, 1058-1063.

Wong, P. T. T., Goldstein, S. M., Grekin, R. C., Godwin, T. A., Pivik, C., and Rigas, B. (1993_c) Distinct infrared spectroscopic patterns of human basal cell carcinoma of the skin. Cancer Res., **53**, 762-765.

Wong, P. T. T., Lacelle, S., Fung, M. F. K., Senterman, M., and Mikhael, N. Z. (1995) Characterization of exfoliated cells and tissues from human endocervix and ectocervix by FTIR and ATR/FTIR spectroscopy. Biospectroscopy, **1**, 357-364.

Yesner, R. (1978) Spectrum of lung cancer and ectopic hormones. Pathology Annals, **13**, 217-241.

APPENDIX A

Theory of Fourier Transform Infrared Spectroscopy

A.1 Principles of Infrared Spectroscopy

Infrared spectroscopy is the study of the interaction of infrared light with matter. Light is a form of electromagnetic energy consisting of perpendicular oscillating electric and magnetic fields. The electric part of the light wave, known as electric vector, interacts with molecules. The wavelength of a light wave is the distance between adjacent crests or troughs and is denoted by the symbol lambda (λ). The wavenumber of a light wave is defined as the reciprocal of the wavelength and is given by the equation as follows:

$$\nu = \frac{1}{\lambda}$$

where ν is wavenumber. Here λ is measured in cm, whereas ν is measured as cm^{-1}. ν is a measure of the number of waves (counted as the number of crests or troughs) in a centimeter. The wavenumber of a light wave is directly proportional to energy as follows,

$$E = hc\nu$$

where E = Light energy

c = Speed of light ($3x10^{10}$ cm/second)

h = Planck's constant ($6.63x10^{-34}$ joule-second)

ν = Wavenumber (cm^{-1})

Thus, high wavenumber light has more energy than low wavenumber light (Smith, 1996).

The infrared region of the electromagnetic spectrum lies between the visible and microwave regions. In terms of wavenumber, this region is between 400 cm^{-1} and 4000 cm^{-1}. All molecules are composed of atoms linked by chemical bonds. Infrared absorption bands can be related to the motions of the individual atoms that comprise a molecule. Distinct motions should result in distinct absorption bands. The molecules in a sample will absorb infrared radiation of the appropriate frequency and consequently be excited from one vibrational or rotational state to another. The movement of atoms and chemical bonds is similar to that of a system comprised of springs and balls in constant motion. Their motion can be regarded as being composed of two components, the stretching and bending vibrations. The frequencies of such vibrations are not only dependent on the nature of the particular bonds themselves, but are also affected by the entire molecule and its environment. The vibrations of bonds, which accompany electric vibrations, will increase their amplitude if an electromagnetic wave (infrared beam) strikes them. The difference between a molecule and the spring-ball system is that the vibrational energy levels of the molecule are quantized; therefore only the infrared beam with a frequency exactly corresponding to that required to raise the energy level of a bond will be absorbed (Nakanishi and Solomon, 1977). However, not all bonds in a molecule are capable of absorbing infrared energy, even if the frequency of the radiation exactly matches that of the bond motion. Only those bonds which have a dipole moment that changes during the vibration are capable of absorbing infrared radiation.

A.2 Molecular Vibrations and Characteristic Absorption Bands

When the sample is irradiated by an infrared beam whose frequency is changed continuously, the molecule will absorb certain frequencies as the energy is consumed in stretching or bending different bonds (Nakanishi and Solomon, 1977). The transmitted beam corresponding to the region of absorption is weakened, and thus a recording of the intensity of the transmitted infrared beam versus wavenumbers will give a curve showing absorption bands. This is the infrared spectrum. This allows us to identify the structure of unknown molecules from the molecule's infrared spectrum and their conformation and orientation with respect to the other molecules present in a sample (Smith, 1996).

There are two types of normal vibrational motions in a molecule: the stretching and the bending modes. When the vibratory motion involves alternate stretching and compression along the bond, it is called a stretching vibration. This is explained in Figure A.1 which shows three atoms linked together in a nonlinear fashion. The motion is symmetric where the two end atoms move in and out in phase but they remain in the same bond axis. It can be an asymmetric motion where one atom moves in and the other moves out in alternate direction. A system of three atoms can also undergo a bending motion where the two end atoms change their positions with respect to their original bond axis. In-plane bending vibrations include rocking and scissoring modes. Out-of-plane bending vibrations include wagging and twisting modes.

Figure A.1 Vibrations of a group of atoms (+ and - signify vibrations perpendicular to the plane of the paper) (Nakanishi and Solomon, 1977).

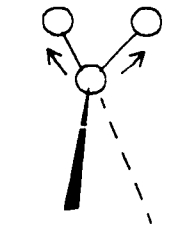

Symmetric

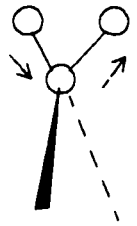

anti-symmetric

STRETCHING VIBRATIONS

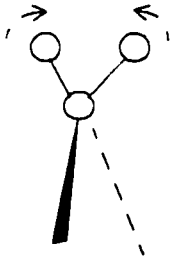

Scissoring

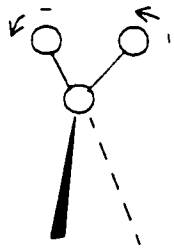

Rocking

IN-PLANE BENDING VIBRATIONS

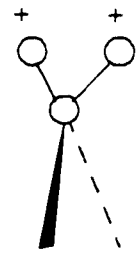

Wagging

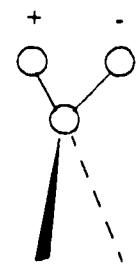

Twisting

OUT-OF-PLANE BENDING VIBRATIONS

Drawing from the classical spring-mass analogy, the stretching frequency ν (cm^{-1}) of a diatomic molecule composed of atoms of masses m_a and m_b can be expressed by the following equation:

$$\nu = \frac{1}{2\pi c}\sqrt{\frac{k(ma+mb)}{m_a m_b}}$$

where c is the velocity of light, and k is the force constant (bond strength in dynes/ cm).

The vibrational motions and frequencies of a structure containing several balls (atoms) of various masses connected by springs (bonds) with various force constants can also be obtained using classical mechanics. It can be seen that the position of a particular bond is determined by the bond strength and mass of the atoms linked by the bond (Lambert *et al.*, 1987). For example, in the case of stretching frequency, the stronger the bonds and the smaller the masses, the higher the absorption frequency of that particular bond. This means that more energy is required to vibrate the bond. Thus a bond of higher order absorbs at higher frequency, provided the masses of the bonded atoms are identical. Generally, the heavier the atoms concerned, the lower the frequency. In a qualitative sense the bending frequencies can also be treated in the same fashion. The results of these calculations are very important because they form the basis for the interpretations of vibrational spectra (Nakanishi and Solomon, 1977).

The movements of the atoms in a molecule may be very complex and is composed of 3N-6 normal modes of vibration for a non-linear molecule, where N represents the number of atoms. This is explained as follows: the movement of an atom in space can

be represented by 3 independent mutually perpendicular movements parallel to the x, y and z axes in a cartesian system. Thus, a system of N free-moving atoms will have 3N independent motions. However, when the atoms are connected together in a molecule, the motions are no longer independent. Three motions become translations of the molecule, where all atoms move simultaneously in the x, y or z directions. Another three are rotations, where all atoms rotate in phase about the x, y and z axes. This leaves 3N-6 motions, in which internuclear distances and bond angles change, but the centre of gravity of the molecule does not move (Lambert *et al.*, 1987). For strictly linear molecules, such as carbon dioxide, the number of normal vibrations is 3N-5. A linear molecule only has two independent rotational degrees of freedom about two mutually perpendicular axes, perpendicular to the molecular axis.

A.3 Fourier Transform Infrared Spectrometers

The core of Fourier Transform Infrared Spectrometer (shown in Figure A.2) is an interferometer named after the inventor A. Michelson. The instrumentation consists of two plane mirrors, one fixed (M1) and one movable (M2) mirror plus a semireflecting beamsplitter. A collimated beam of light from the IR source strikes the beamsplitter, where half the radiation is reflected to mirror M1 and the other half transmitted to mirror M2. After reflection at the mirrors, the two beams recombine at the beamsplitter where again 50% of each is reflected and 50% transmitted.

The fixed and the moving mirror in its dotted position are equidistant from the beamsplitter. The distance traversed by the light beam is the same and the condition is known as zero path difference. In the case of the Michelson interferometer, an optical

Figure A.2 Simplified layout of an FTIR spectrometer system.

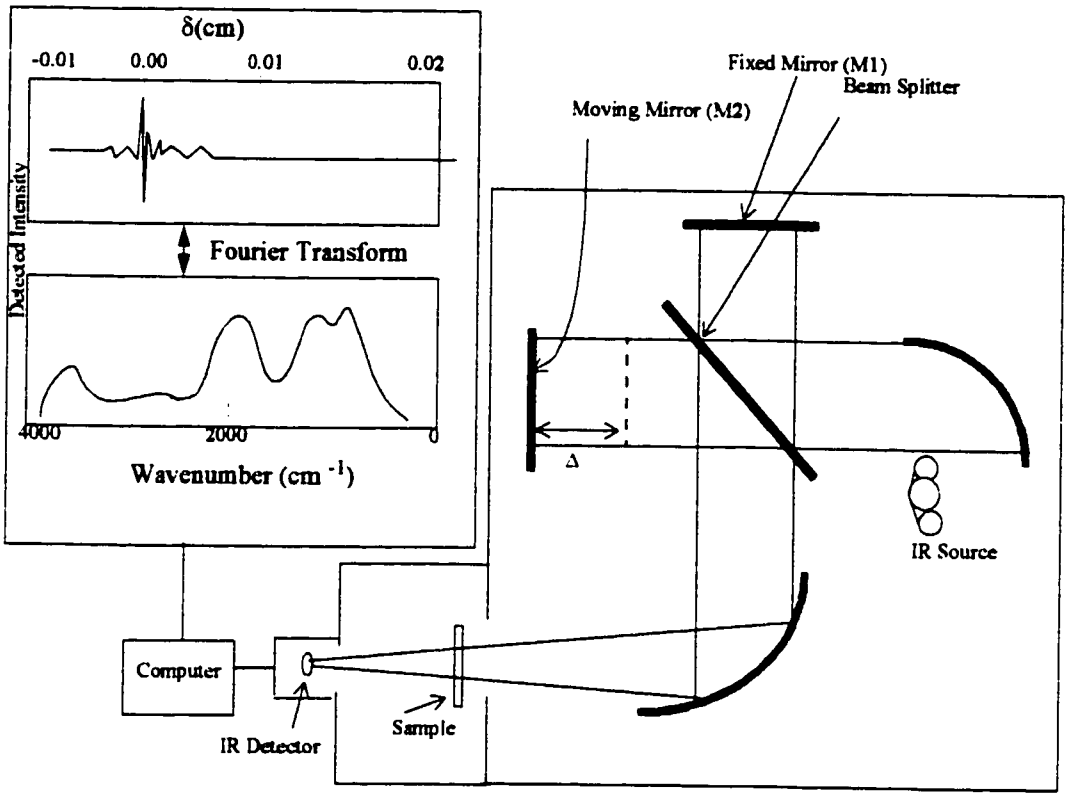
δ(cm)
-0.01
0.00
0.01
0.02
Detected Intensity
Fourier Transform
4000
2000
0
Wavenumber (cm -1)
Fixed Mirror (M1)
Beam Splitter
Moving Mirror (M2)
Δ
IR Source
Computer
IR Detector
Sample

path difference is introduced between the two light beams by moving the mirror M2 away from the beamsplitter. The distance that M2 is moved from its dotted position (Zero path difference) in Figure A.2 is called the mirror displacement and is denoted by the symbol Δ. The optical path difference δ is related to Δ by $\delta=2\Delta$ since the light reflecting off the moving mirror M2 travels a distance Δ on the way to the mirror and a distance Δ on its return trip to the beamsplitter.

The principle of the spectrometer can be explained simply by considering a monochromatic source of wavelength λ. If the path difference δ is zero or an integral multiple of λ, the two beams that recombine at the beamsplitter are in-phase. The signal at the detector will be of maximum intensity due to constructive interference. Mathematically speaking, $\delta=n\lambda$ where 'n' is any integer with the values n=0,1,2,3...

If δ has any other value, the two beams of light will be partially out-of-phase, resulting in destructive interference and decreased detector signal. The optical path differences for complete destructive interference is given by: $\delta=(n+1/2)\lambda$ where n=0,1,2,3... (Smith, 1996).

When the movable mirror 'M2' moves at a constant velocity 'u' through some distance r, the signal received at the detector will be a cosine wave whose frequency is given by $f=u/\lambda=u\nu$, where ν is the wavenumber frequency of the incident radiation. The amplitude or intensity of this signal as a function of 'δ' is denoted by $I(\delta)$ and is termed an interferogram. This function is proportional to $\cos(2\pi\nu\delta)$.

In the case of polychromatic light, all frequencies will be in-phase only at zero path difference ($\delta=0$). Various degrees of destructive interference occur at any other δ. The interferogram $I(\delta)$ resulting from one sweep of moving mirror M2 will be proportional to

the sum of the intensities of all the interfering wavelengths, $\Sigma_i A_i \cos(2\pi\nu_i\delta)$ where A_i is the maximum amplitude of the cosine for each incident frequency, ν_i. For a continuous incident spectrum, 'i' is infinite and an integral used in place of the sum. This interferogram I (δ) has maximum amplitude at δ=0 (Susi and Byler, 1986).

A sample is placed between the interferometer and the detector which reduces the intensity of radiation at any frequency at which the sample absorbs energy. The interferogram is then mathematically manipulated to yield an absorption spectrum by computer based discrete Fourier transform.

The characteristics of the IR beam incident on the sample is obtained from the interferogram taken without the sample. This is commonly referred to as blank spectrum $I_b(\nu)$. Absorbance spectra are calculated from single-beam intensity spectra measured with the sample $I_s(\nu)$ and with a blank $I_b(\nu)$ respectively, using the formula $A(\nu)= -\log_{10} [I_s(\nu)/I_b(\nu)]$ (Braiman and Rothschild, 1988).

A.4 Fourier Self-Deconvolution and Spectral Derivation

Fourier self-deconvolution is a mathematical means for reducing bandwidths so that overlapped bands can be resolved from one another. This method is also used to enhance the resolution of the spectrum. It is most commonly performed on a section of the spectrum where several narrower bands overlap to give a broad band. The deconvolution process helps us to determine the number and positions of overlapped bands. This type of data processing does not increase the instrumental resolution, but it does increase the degree to which the individual component bands can be visualized. The band-narrowing during deconvolution process is achieved at the expense of some distortion of the original

spectral band shape and leads to a degradation of the signal-to-noise ratio, which involves a certain degree of subjectivity (Tooke, 1988).

The mathematical basis for Fourier self-deconvolution is set by approximating the infrared spectral peak to be Lorentzian in form (Figure A.3 (a)). Mathematically, spectral peak E(ν) is represented by

$$E(\nu) = \frac{\sigma}{\pi[\sigma^2 + (\nu - \nu_O)^2]}$$

where ν_0 is the center frequency of the peak and σ represents the Lorentzian half-width at half-maximum. The Fourier transform of E(ν) is given by a damped cosine function in Figure A.3 (b).

$$I(\delta) = [\exp(-2\pi\sigma|\delta|)]2\cos(2\pi\nu_O\delta)$$

The next step is to deconvolve the transform so that the profile determining the bandwidth is removed. This is done by multiplying the above equation with a rising exponential $\exp(2\pi\sigma|\delta|)$ which cancels out the damping to leave a cosine train of constant amplitude (c). If this result is continuous, i.e. the train extended to infinite distance x, the transformation would yield a single line (d) in place of the original peak (a). In reality of course, data sets are finite in extent (Figure A.3 (e)). The interferogram and the Fourier integral must be truncated at some finite point. The limits of integration are the zero path difference and measures the maximum optical path difference. Transformation in this case results in a peak (Figure A.3 (f)) which is much narrower than the original peak, (Figure A.3 (a)), but with complication of sinusoidal side-lobes. In order to eliminate

Figure A.3 Some basic processes in Fourier self-deconvolution (Tooke, 1988).

(a) Single spectral peak represented by a Lorentzian function in wavenumber domain.
(b) The transform of (a) shown as an exponentially damped cosine train.
(c) Multiplication of (b) by a rising exponential gives a cosine train of constant amplitude.
(d) Transform of (c) yields single peak in place of original peak.
(e) Cosine train of (c) is limited from zero path difference to maximum path difference.
(f) Transformation of (e) yields (f) much narrower than (a) but with sidelobes.
(g) The cosine train is scaled with an apodisation function.
(h) Transform of (g) yields a smooth band without sidelobes.

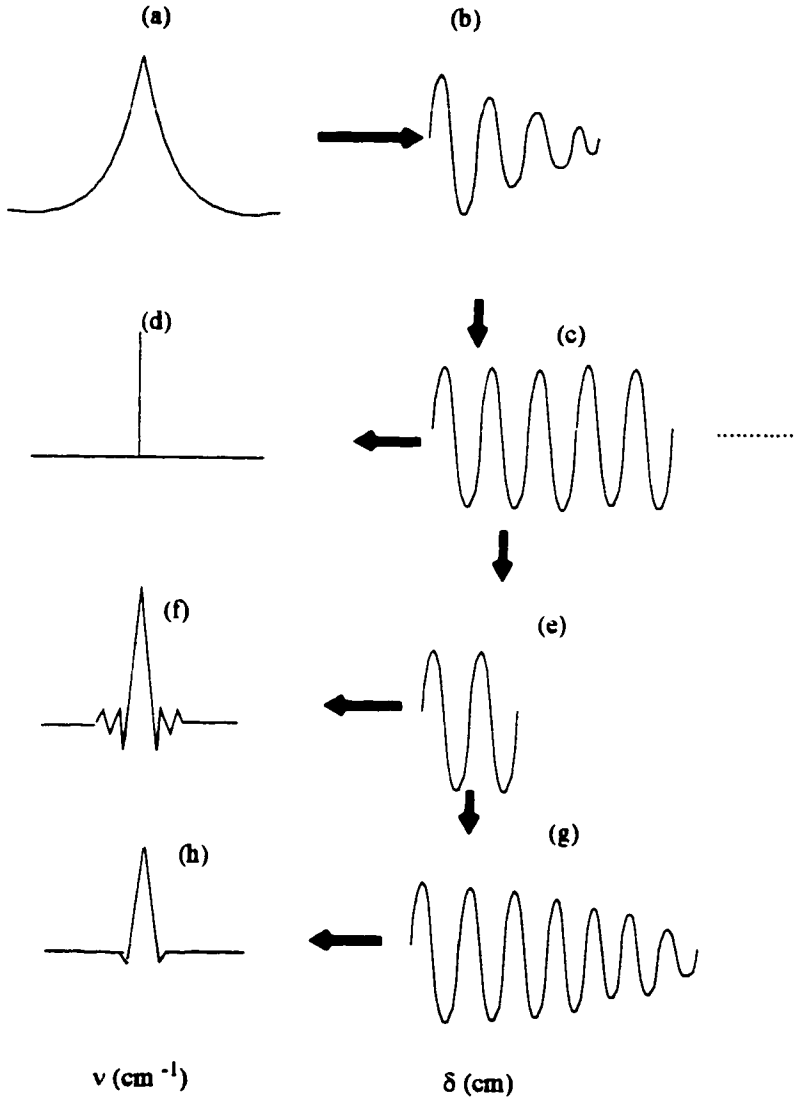
(a)
(b)
(d)
(c)
(f)
(e)
(h)
(g)
ν (cm -1)
δ (cm)

these undesirable artifacts, the cosine train is scaled with an apodisation function (Figure A.3(g)) which terminates at some defined point, the final result (Figure A.3(h)) being a smooth band with little sign of side-lobes and narrower than original (a).

The user can control the steps of Fourier self-deconvolution and hence determine the final outcome by inputting certain information. In order to define the deconvoluting exponential, an estimate of bandwidth is necessary. Next, the degree to which the band is narrowed is chosen, which choice incidentally largely defines the truncation point. Finally, the apodisation point must be selected. Choice of apodisation function is dictated by two generally contradicting constraints: the noise present in the original spectrum, and how acceptable small side-lobes will be in the result. Fourier self-deconvolution programs are therefore interactive and iterative in nature, with the operator varying parameters so as to converge towards what he/she judges to be a sensible result (Tooke, 1988; Griffiths and Pariente, 1986)

Derivation is another tool applied in infrared spectroscopy to permit identification of individual features in complex absorption contours. This technique can also be applied in both the wavenumber and Fourier domains. In the wavenumber domain, derivative routines calculate the rate of change of the slope of the composite band directly from the spectrum (Jackson *et al.*, 1989). The derivative of a spectrum can be taken 'n' number of times, producing derivatives of different orders. For instance, the first derivative of a spectrum is called a first order derivative, the derivative of the first derivative is called second order derivative and so on. Fourier derivative routines apply a weighing function $(i2\pi\delta)^n$ to the Fourier transform of the spectrum (n-order of the derivative). This may be directly compared with the function used in deconvolution, which is exponential for

Lorentzian lines. Derivation also requires high signal-to-noise ratio of the spectrum (Smith, 1996; Cameron and Moffatt, 1984). Ideally, the power of the derivative is kept at the default value of 3 with a smoothing breakpoint in the range 0-1 for our analysis.

Appendix B

Table B.1: Assignment of the major infrared bands in tissue samples spectra [a]

Frequency (cm^{-1})	Vibrational[b] Mode	Major Contribution
3015	ν=CH	Lipids
2959	$\nu_{as}CH_3$	Lipids and proteins
2925	$\nu_{as}CH_2$	Lipids
2854	ν_sCH_2	Lipids
1655	Amide I	Proteins
1642	δOH	Water
1549	Amide II	Proteins
1467	δCH_2	Lipids
1457	$\delta_{as}CH_3$	Collagen
1454	$\delta_{as}CH_3$	Proteins
1404	δ_sCH_3	Collagen
1401	δ_sCH_3	Proteins
1283-1339	?	Collagen
1242	Amide III	Collagen
1238	$\nu_{as}PO_2^-$	Nucleic acids
1205	?	Collagen
1156-1172	νC-O	Glycogen and Proteins
1122	νC-O	Mucin
1082	$\nu_sPO_2^-$	Nucleic acids
1052	νC-O+δC-O	Glycogen
1043	νCH_2OH	Mucin
1031	?	Collagen
1025	νCH_2OH	Glycogen
971	$\nu_2PO_4^-$	Nucleic acids and proteins

a. Adapted from Wong *et al.*, 1995.

b. ν represents stretching mode and δ denotes bending mode.

CURRICULUM VITAE

Name: Vanisree Kathiravan

Address: 1811, Stearns Hill Road,
Waltham, MA 02451,
U.S.A.

Telephone (781)-899-5983

Education:

M.Sc., Biochemistry
University of Ottawa (1995-1999)
M.Sc., Biochemistry
PSG College of Arts and Science (1991-93)
B.Sc., Biochemistry
Avinashilingam Deemed University (1988-91)

Experience:

Medical Biochemist
Institute of Laboratory Sciences
Kovai Medical Center (1994)
India

ABSTRACTS/PRESENTATIONS:

1. **Kathiravan, V.**, Belbaraka, L., Siddiqi, S., Jouishomme, H., Phipps, J., Wong, P.T.T., and Carrier, D. 1998. The diagnostic test based on Fourier transform infrared spectra of quiescent tumor cells efficiently monitors their ability to proliferate. Presented as a poster at the 4th International Symposium on Predictive Oncology and Therapy, France, Oct. 24-27, 1998.